Lab on a Chip

Integrating Microfluidic and Bioprinting Technologies: Advanced Strategies for Tissue Vascularization

Journal:	*Lab on a Chip*
Manuscript ID	LC-TRV-03-2024-000280.R1
Article Type:	Tutorial Review
Date Submitted by the Author:	14-Aug-2024

Complete List of Authors:	Mei, Xuan; Harvard Medical School, Yang, Ziyi; Harvard Medical School, Medicine Wang, Xiran; Harvard Medical School, Medicine Shi, Alan; Brookline High School Blanchard, Joel; Icahn School of Medicine at Mount Sinai Elahi, Fanny; Icahn School of Medicine at Mount Sinai Kang, Heemin; Korea University - Seoul Campus, Materials Science and Engineering (joint: College of Medicine) Orive, Gorka; University of the Basque Country, Pharmaceutical Technology; Biomedical Research Networking Center in Bioengineering, Biomaterials and Nanomedicine, CIBER-BBN, Zhang, Yu Shrike; Harvard Medical School, Medicine

Integrating Microfluidic and Bioprinting Technologies: Advanced Strategies for Tissue Vascularization

Xuan Mei[1], Ziyi Yang[1,2], Xiran Wang[1,3] Alan Shi[4], Joel Blanchard[5], Fanny Elahi[5,6], Heemin Kang[7,8,*], Gorka Orive[9,10,11,12,13,*], Yu Shrike Zhang[1,*]

[1]Division of Engineering in Medicine, Department of Medicine, Brigham and Women's Hospital, Harvard Medical School, Cambridge, MA 02139, USA

[2]School of Biological Science, University of California Irvine, Irvine, CA 92697, USA

[3]Department of Mechanical and Aerospace Engineering, University of California, San Diego, San Diego, CA 92161, USA

[4]Brookline High School, Brookline, MA 02445, USA

[5]Departments of Neurology, Neuroscience, and Pathology, Icahn School of Medicine at Mount Sinai, New York, NY 10029, USA

[6]James J. Peters Department of Veterans Affairs Medical Center, Bronx, NY 10468, USA

[7]Department of Materials Science and Engineering, Korea University, Seoul 02841, Republic of Korea

[8]College of Medicine, Korea University, Seoul 02841, Republic of Korea

[9]NanoBioCel Research Group, School of Pharmacy, University of the Basque Country (UPV/EHU), Vitoria-Gasteiz, Spain

[10]Bioaraba, NanoBioCel Research Group, Vitoria-Gasteiz, Spain

[11]Biomedical Research Networking Centre in Bioengineering, Biomaterials and Nanomedicine (CIBER-BBN), Vitoria-Gasteiz, Spain

[12]University Institute for Regenerative Medicine and Oral Implantology - UIRMI (UPV/EHU-Fundación Eduardo Anitua), Vitoria-Gasteiz, 01007, Spain

[13]Singapore Eye Research Institute, Singapore 169856, Singapore

[*]Corresponding authors. Emails: yszhang@bwh.harvard.edu (Y.S.Z.); gorka.orive@ehu.eus (G.O.) heeminkang@korea.ac.kr (H.K.)

Abstract

Tissue engineering offers immense potential for addressing the unmet needs in repairing tissue damage and organ failure. Vascularization, the development of intricate blood vessel networks, is crucial for the survival and functions of engineered tissues. Nevertheless, the persistent challenge of ensuring an ample nutrient supply within implanted tissues remains, primarily due to the inadequate formation of blood vessels. This issue underscores the vital role of the human vascular system in sustaining cellular functions, facilitating nutrient exchange, and removing metabolic waste products. In response to this challenge, new approaches have been explored. Microfluidic devices, emulating natural blood vessels, serve as valuable tools for investigating angiogenesis and allowing the formation of microvascular networks. In parallel, bioprinting technologies enable precise placement of cells and biomaterials, culminating in vascular structures that closely resemble the native vessels. To this end, the synergy of microfluidics and bioprinting has further opened up exciting possibilities in vascularization, encompassing innovations such as microfluidic bioprinting. These advancements hold great promise in regenerative medicine, facilitating the creation of functional tissues for applications ranging from transplantation to disease modeling and drug testing. This review explores the potentially transformative impact of microfluidic and bioprinting technologies on vascularization strategies within the scope of tissue engineering.

1. Introduction

Tissue engineering, the interdisciplinary field where biology, engineering, and medicine converge, holds the promise of addressing the critical challenges posed by tissue damage and organ failure.[1–4] As a multidisciplinary field, tissue engineering combines branches of cell biology, molecular biology, materials science, chemistry, and engineering.[5–7] The main task of tissue engineering is to reproduce the structures and functions of living tissues by designing the architectures of biocompatible materials with advanced technologies to replicate predetermined cell responses and drive consequent biological processes.[8–11] Tissue engineering can help advance understanding of disease processes as well as provide novel therapeutic angles.

One of the current limitations of tissue engineering is its inability to form a functional vascular network in the initial phase.[12–15] In nature, the vascular system of the human body is comprised of a large number of vessels, including arteries, veins, and capillaries.[16,17] The vascular system provides an essential molecular and cellular transport and inter-organ communication network throughout the body,[18–20] which maintains cellular functions (growth and development),[21,22] allows absorption of essential nutrients (such as vitamins and minerals),[23,24] and enables removal of cellular and metabolic waste products.[25–27] This critical aspect, vascularization, is vital to sustaining tissue vitality and proper functions.[28,29] As tissue constructs increase in size and complexity, a fundamental requirement emerges for a natural-like, perfusable network of blood vessels that can effectively deliver oxygen, nutrients, and regulatory signals to each cell within the engineered tissue.[30–32] Without a functional vascular network, the cells in the innermost layers of an engineered tissue may remain deprived of the essential resources it needs to thrive.[33–35]

Over the years, researchers have explored many approaches to address the challenges of vascularization in engineered tissues.[36–39] Microfluidic devices, capable of mimicking the dynamic fluid flow and structural complexity of natural blood vessels, have emerged as a collection of powerful tools for studying angiogenesis and guiding the formation of microvascular networks.[40–42] Meanwhile, bioprinting empowers researchers to precisely place cells or/and biomaterials in three-dimensional (3D) patterns, creating intricate vascular architectures that closely mimic the native vessels.[43,44] The convergence of microfluidic and bioprinting technologies has ushered in a new era of innovation in vascularization strategies.[45,46] From microfluidic bioprinting to creating perfusable organ-on-a-chip systems, researchers are pushing the boundaries of tissue vascularization.[47–50] These advancements hold profound implications for disease modeling,

regenerative medicine and drug discovery, [51–53] enabling the fabrication of functional tissues that can potentially be transplanted,[54,55] incorporated into disease models,[56,57] or deployed for drug testing.[44,58]

In this review, we journey through the evolving landscape of strategies, techniques, and breakthroughs in exploring vascularization in tissue engineering. We delve into the principles of angiogenesis, the recent development of microfluidic and bioprinting technologies, along with their integration. We also examine the innovative ways researchers harness them for vascularization (**Fig. 1**). Ultimately, the challenges for developing vascularization technologies in tissue engineering are discussed.

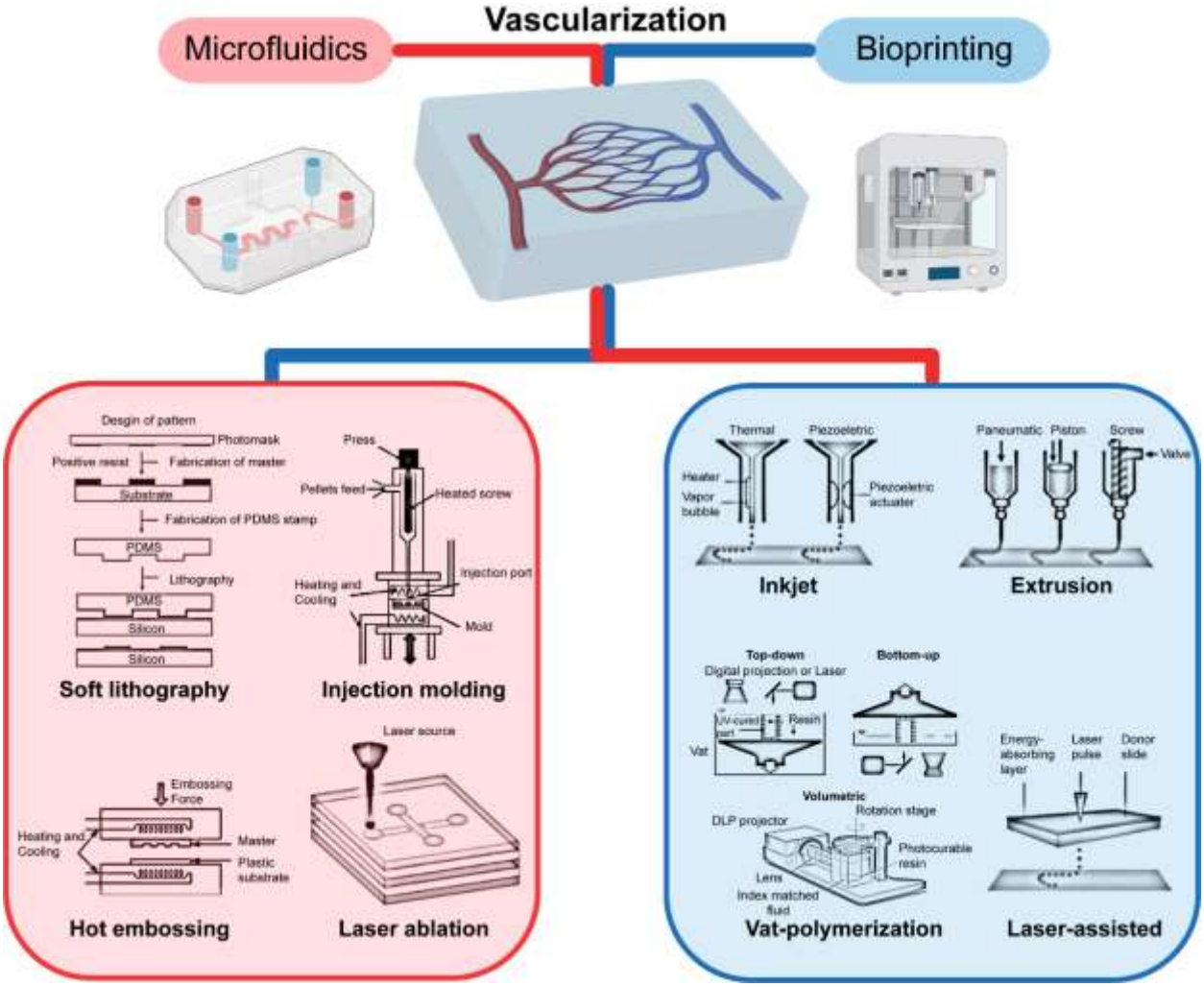

Fig. 1. Major microfluidic and bioprinting technologies used to mimic tissue vascularization. Reproduced with permission from ref. 59–63.[59–63] Created with BioRender.com.

2. Blood vessels and tissue engineering

2.1 Biology of native blood vessels

2.1.1 Structure of native blood vessels

The structure of the native small blood vessels can be classified into three parts: arteries, veins, and capillaries.[64,65] These structures allow blood to be transported through the entire body.[66] Artery, sometimes termed elastic artery when closer to the heart and macular artery when far away, consists of three layers: tunica intima, tunica media, and tunica externa.[67] Tunica intima has three layers: endothelium, basal lamina, and connective tissue layer.[27,68] The tunica media layer can be divided into connective tissue, elastic fiber, and smooth muscle.[69] Between the tunica media and tunica externa, external elastic lamina exists.[70,71] Tunica externa comprises connective tissues, most of which are collagenous fibers.[72,73] Similar to arteries, the walls of veins are composed of the same three layers but with less smooth muscle and connective tissue.[74]

Capillaries can be categorized into continuous capillaries, fenestrated capillaries, and sinusoidal capillaries.[75,76] Capillaries are approximately 5 to 10 μm in diameter and are made of only two layers of cells.[77–79] The wall of the inner layer is made of endothelial cells with a basement membrane surrounding it;[80,81] the outer layer is composed of epithelial cells.[82,83] The main difference between the three categories of capillaries can be explained by the size of substances that can pass through the capillaries.[84] Due to the unique endothelial layer and intercellular cleft structure, continuous capillaries allow only small substances, such as glucose and water, to pass through.[85] Unlike continuous capillaries, fenestrated capillaries possess pores within their endothelial layers, effectively filtering larger substances.[86,87] The largest substances, such as cells and plasma proteins, can only pass through sinusoid capillary due to an intercellular gap and incomplete basement membrane.[88,89]

2.1.2 *In vivo* formation of native blood vessels: vasculogenesis and angiogenesis

The formation of the native blood vessels features mainly two stages: vasculogenesis and angiogenesis.[90] The process of blood vessel formation is termed “vasculogenesis”.[91,92] Native blood vessels form during the 3rd week of embryo development.[93] The early structure of the embryo is formed from the embryonic mesoderm, where mesenchymal cells will differentiate into the connective tissue and the smooth muscle of the blood vessel.[94,95] Blood islands, which consist of a clump of small cells named “hemangioblasts”, are responsible for the early production of the blood vessels and primitive blood cells.[96,97] The hemangioblasts produce different types of cells,

such as blood and endothelial cells.[98] Vascular cords form when endothelial cells connect with different blood islands, which serve as the precursor of the mature blood vessels.[99] Different from vasculogenesis, which occurs only in the embryonic state, angiogenesis occurs both in the embryonic state and postnatally.[100] The angiogenesis process can be separated into two processes: sprouting angiogenesis and intussusceptive angiogenesis.[101] Sprouting angiogenesis occurs when one endothelial cell becomes activated by the vascular endothelial growth factor type A (VEGF-A) stimulation and transforms into tip cells.[102] New blood vessels form as the tip cells move with the stimulation from VEGF-A.[103,104] Intussusceptive angiogenesis happens when the blood vessels split from one into two, causing transvascular tissue pillars to form and expand.[105,106]

2.2 Materials used for scaffold fabrication in tissue engineering

Materials used for scaffold production should be biocompatible, biodegradable, nontoxic, and able to mimic the local extracellular matrix (ECM) with specific features such as density, stiffness, viscoelasticity, degradation, and integrin-binding motifs.[107–110] Either natural or synthetic polymers have been studied for scaffold fabrication,[111–113] which are critical regarding their mechanical property and biocompatibility.[114,115] Naturally derived polymers, such as collagen,[116,117] chitosan,[118,119] and gelatin[120,121] are popular in tissue engineering because of their biocompatibility.[122,123] Different formula have been developed to address the limitations of naturally derived polymers.[124,125] Unlike naturally derived polymers, synthetic polymers exhibit better mechanical strength, better consistency, and more flexibility in the design.[126–131] In this review, we will not delve into the details of the materials since they are extensively discussed in other reviews.[132–136]

3. Microfluidic technologies

Within the microscale, microfluidic devices have been intricately designed to address the challenges encountered in research conducted using conventional *in vitro* and *in vivo* models, offering distinct benefits, including high-throughput tests with decreased consumption of regents.[137,138] Through their adept mimicry of blood vessels and angiogenesis, these systems empower researchers to meticulously recreate organ physiology by adroitly manipulating various factors of microscale physics over distances, mechanical cues, tissue arrangements, and geometries.[139,140] Here, we summarize the general fabrication methods for microfluidic systems, focusing on the technical aspects, and then explore their applications in vascularization.

3.1 General microfluidic technologies

3.1.1 Soft lithography

As one of the most favored approaches for crafting biomedical microfluidic devices, soft lithography developed rapidly from 1995 to 2005,[141] which employs elastomeric substances for replica molding and creates patterns essential for microfluidic device fabrication.[142] In soft lithography, a molded elastomeric pattern is positioned onto a liquid prepolymer solution, which subsequently undergoes polymerization, forming corresponding hydrogel features.[143] During this procedure, the liquid material occupies the intricate patterns on the elastomeric replica due to the effects of surface tension and capillary flow.[144]

Unlike conventional photolithography, soft lithography creates microscale or nanoscale structures regardless of the substrates, which especially surmounts the prevalent limitations associated with photolithography in biological and biomedical contexts.[145] Although soft lithography offers significant advantages in terms of flexibility and ease of replication, its use is somewhat limited by the durability and material constraints of soft materials, which may degrade or deform over time.[146] Among all the materials used for soft lithography, polydimethylsiloxane (PDMS) has risen to prominence. Researchers esteemed it for its attractive attributes in prototype fabrication: cost-effectiveness, optical, biocompatibility, safety, accessible molding procedures, and the capacity for integrating elastomeric actuators and optical components into devices.[147,148] The superior sealing capabilities of PDMS render it highly suited for microfluidics applications, while its self-bonding capability facilitates the construction of multilayer structures.[149]

3.1.2 Micromolding

Utilizing specialized molds, micromolding emerges as an intricate technique for shaping plastic polymers, such as cyclic olefin polymer (COC) and polystyrene (PS).[150] The micromolding process can be divided into four steps: fabricating the mold containing the desired pattern, applying polymer material, curing polymer material, and extracting the cured polymer from the mold.[151] The most common micromolding techniques are injection molding,[152] hot embossing,[153] and laser ablation.[154]

3.1.2.1 Injection molding

Termed as injection molding, the material (usually polymer) is molten and injected into a mold, solidifying into the desired part shape after cooling down.[152] Injection molding is the leading manufacturing process for microfluidic device fabrication due to its high production efficiency.[155]

Moreover, the accuracy and consistency of injection molding are of great significance for massive production. However, only thermoplastics can be used for injection molding. For example, PS is commonly used for cell growth,[156] and COC is known for its favorable optical properties for microscopes.[157]

3.1.2.2 Hot embossing

Particularly valuable for thermoplastic materials, hot embossing presents a cost-effective approach for high-throughput manufacturing.[153] The process itself involves three key stages: positioning the polymer film between the molds, elevating both film and molds to temperatures surpassing the polymer's glass-transition point within a vacuum, pressing the molds onto the softened polymer to effectuate feature transfer, and finally cooling all components below the polymer's glass-transition temperature for demolding and completion of the process.[158] With a widespread presence in plastics manufacturing, hot embossing is particularly useful for high aspect ratio structures, which enables the translation of microfluidic cell culture devices with micro- and nanoscale features from laboratory to clinical studies.[159] However, the size of channels created by hot embossing is still limited due to the thermal stresses during the process.

3.1.2.3 Laser ablation

With the high demand for more precise and manageable methods to construct microfluidic channels, laser processing has emerged as a potent strategy.[160] Laser ablation can be described as breaking the chemical bonds of materials when interacting with laser light, increasing temperature and pressure to create voids on the substrates.[161] Laser systems, such as the CO_2 laser,[162] and the diode laser,[163] are commonly used. While different types of laser sources will affect the ablation process, the properties of the substrate materials, such as reflectance, thermal conductivity, and absorption coefficient, also play a significant role in fabrication. Polymers, such as polytetrafluoroethylene (PTFE)[164] and poly(methyl methacrylate) (PMMA),[165] have been explored for the fabrication of microfluidic devices using laser ablation. The high precision and control make laser ablation suitable for other materials including metals and ceramics.[166] This versatility, combined with the ability to achieve intricate designs, makes laser ablation valuable for applications requiring detailed patterning. However, laser ablation involves high equipment and maintenance costs. Additionally, achieving uniform depth over large areas can be challenging.

3.2 Microfluidic technologies for vascularization

3.2.1 Soft lithography

Soft lithography has been applied to create microfluidic vessel structures integrated within certain matrices to mimic different tissues.[143] As an example, the focus of cardiac tissue engineering is replacing damaged contractile tissue and emulating cardiac diseases for therapeutic purposes. However, integrating aligned contractile tissue and perfusable vasculature remains challenging. For instance, it was demonstrated the successful introduction of vascular lumens into matrix-contracting cardiomyocytes.[167] In this work, low-density collagen hydrogel was used to generate dense contractile human embryonic stem cell-derived cardiomyocytes (hESC-CMs). In comparison, higher-density collagen hydrogel provided a foundation for a patterned microvasculature fabricated from stromal cells. The lithography-patterned microvascular networks maintained their morphology in the densely cardiac constructs for 2 weeks, showing substantial cardiac tissue engineering advancements.

Different polymers have been investigated for soft lithography, among which PDMS is commonly used due to its easy handling and good biocompatibility.[148] A novel manufacturing method has been developed recently, allowing for the efficient and speedy creation of custom microfluidic devices through 3D printing and PDMS soft lithography.[168] This approach has enabled the design, production, and thorough testing of a microfluidic lab-on-chip that could support the growth of capillary-like structures. Natural polymers, such as collagen and gelatin, have also been utilized for scaffold fabrication using soft lithography.[143] For example, a lithographic technique was harnessed for creating endothelialized microfluidic vessels seamlessly integrated within a native collagen matrix.[169] Moreover, the study delved into the intricate angiogenic activities these cultivated endothelial structures demonstrated, and their dynamic interactions with perivascular cells thoughtfully seeded within the collagen bulk.

3.2.2 Micromolding

3.2.2.1 Injection molding

Diverse hydrogel types encapsulating certain types of cells were confirmed to form different geometries for different purposes, such as the specialized high surface area-to-volume spiral configuration explicitly designed for islet macroencapsulation in treatment of type 1 diabetes.[170] Various tissue models, such as the heart, have been created through injection molding. As an example, liquid collagen containing human embryonic stem cell-derived endothelial cells (hESC-ECs) was used during injection modeling to create perfusable constructs with microchannels (**Fig. 2A**).[171] The remodeled constructs featuring vascular anastomosis exhibited increased expressions

of genes linked to vasculature, which contributed to the remodeling of graft cardiomyocytes upon implantation onto an infarcted heart (**Fig. 2B**). The study employed a multidisciplinary approach, offering insights into the complex interplay between engineered tissues and the host environment for therapeutic advancements in cardiac repair. Beyond normal organs, *in vitro* tumor models integrated with vascularized structures are of great interest since tumor microenvironment (TME) is highly related to tumor vascularization.[172] An all-in-one injection-molded plastic array 3D culture platform (All-in-One-IMPACT) was developed, which integrated vascularized tumor spheroids for cancer metastasis mechanistic study (**Fig. 2C**).[173] This model was also tested for drug screening in the metastatic cancer model (**Fig. 2D**). Polymers, such as polycaprolactone (PCL), have been studied for scaffold fabrication as well. As reported, the mass-producing of porous PCL tissue engineering scaffolds was achieved through the combination of microcellular injection molding with chemical foaming and particulate leaching methods.[174] Cell viability assays involving NIH/3T3 fibroblasts demonstrated favorable biocompatibility of the resultant interconnected porous PCL scaffolds, providing a more expansive domain for cell spreading.

3.2.2.2 Hot embossing

Along with the increase in temperature, thermoplastic polymers experience different states, including the glassy state, rubbery state, and flow state.[175] For the fabrication through hot embossing, thermoplastic polymers are the most popular materials because of the low molding temperature and wide range of thermal properties.[158] Made from thermoplastic polymers, well plate-based organ-on-a-chip vascular systems show potential in high-throughput tests through hot embossing. To this end, a 3D vascularized pancreatic adenocarcinoma tissue was developed within a tri-culture system in a 96-well plate comprising patient-derived pancreatic organoids, human fibroblasts, and endothelial cells (**Fig. 2E**).[176] They further applied this technology to create vascularized cardiac, hepatic, and metastatic breast cancer tissues by incorporating patient-derived organoids, termed Integrated Vasculature for Assessing Dynamic Events (InVADE, **Fig. 2F**).[177] This method offers a comprehensive framework for cultivating complex organoids with functional vasculature, such as fibroblast co-cultured tumor organoid (**Fig. 2G**), opening new avenues for dynamic event assessments and personalized medicine applications. Another advantage of hot embossing in fabrication falls in the fabrication of 3D structures through layer-by-layer assembly. Small microchannels were fabricated in a polycarbonate (PC) film using hot embossing, followed by surface functionalization through a crosslinked hyaluronic acid/chitosan layer using layer-by-

layer assembly.[178] Peptides were introduced to enhance adhesion and trigger angiogenesis. The functionalized scaffolds were tested for *in vitro* blood vessel formation, leading to the rapid development of tubular-like structures within 2 hours of incubation. The utilization of hot embossing is oftentimes combined with other fabrication technologies. A technique termed (nano)imprint lithography (NIL) was designed, which utilized both hot embossing and reactive ion etching (RIE) technologies.[179] This novel approach presents a means to fabricate microscale objects using biopolymers, achieved by thermally imprinting on water-soluble sacrificial layers.

3.2.2.3 Laser ablation

Laser ablation can fabricate a network of pores or channels within several hundred micrometers. For example, arrays of small pores were introduced onto the tube walls through focused laser ablation (**Fig. 2H**).[180] This design allowed for cultivating endothelial cells on the inner surfaces of the perforated PDMS tubes within an ECM-like environment. Consequently, the endothelial cells could extend outward through the pores into the surrounding matrix. When two perforated PDMS tubes were positioned parallelly within the matrix, they promoted the development of an interconnected microvasculature or larger vessel network from human umbilical vein endothelial cells (HUVECs, **Fig. 2I**). This network formation appeared to rely on the flow dynamics within the PDMS tubes. Notably, tumor angiogenesis was initiated when co-cultured with tumor spheroids (**Fig. 2J**). Applying perforated and endothelialized PDMS tubes offers a convenient approach for *in vitro* vascular modeling. This advancement is anticipated to contribute to enhanced biological investigations and improved therapeutic screening in the future. Similarly, suturable vascular grafts with microporous structures were created, enabling rapid blood perfusion and enhancing tissue integration.[181] Utilizing electrospinning and femtosecond laser ablation, poly(glycerol sebacate) (PGS)/polyvinyl alcohol (PVA) grafts developed a network of approximately 100-μm pores within tube walls, enabling direct endothelial cell migration towards osteoblasts when incorporated into gelatin methacryloyl (GelMA) hydrogels, thereby facilitating rapid vascularization for bone tissue regeneration.

The accuracy of the laser also allows more precise microstructure fabrication in a microfluidic system. In a recent study, a microfluidic system was introduced that effectively facilitated high-resolution imaging of cargo transport within *in vitro* endothelial models (**Fig. 2K**).[182] Two horizontally separated channels were created for the seeding of human vascular endothelial cells (ECs) and pericytes to emulate the blood-brain barrier. The two types of cells were divided by a

cell growth-enhancing membrane, where a laser-cut observation window was embedded for imaging (**Fig. 2L**). In another study, PGS elastomers were synthesized with different crosslinking ratios, and their surfaces were patterned with channels using laser ablation.[183] Remarkable endothelial cell proliferation and cellular organization were observed on the PGS membranes.

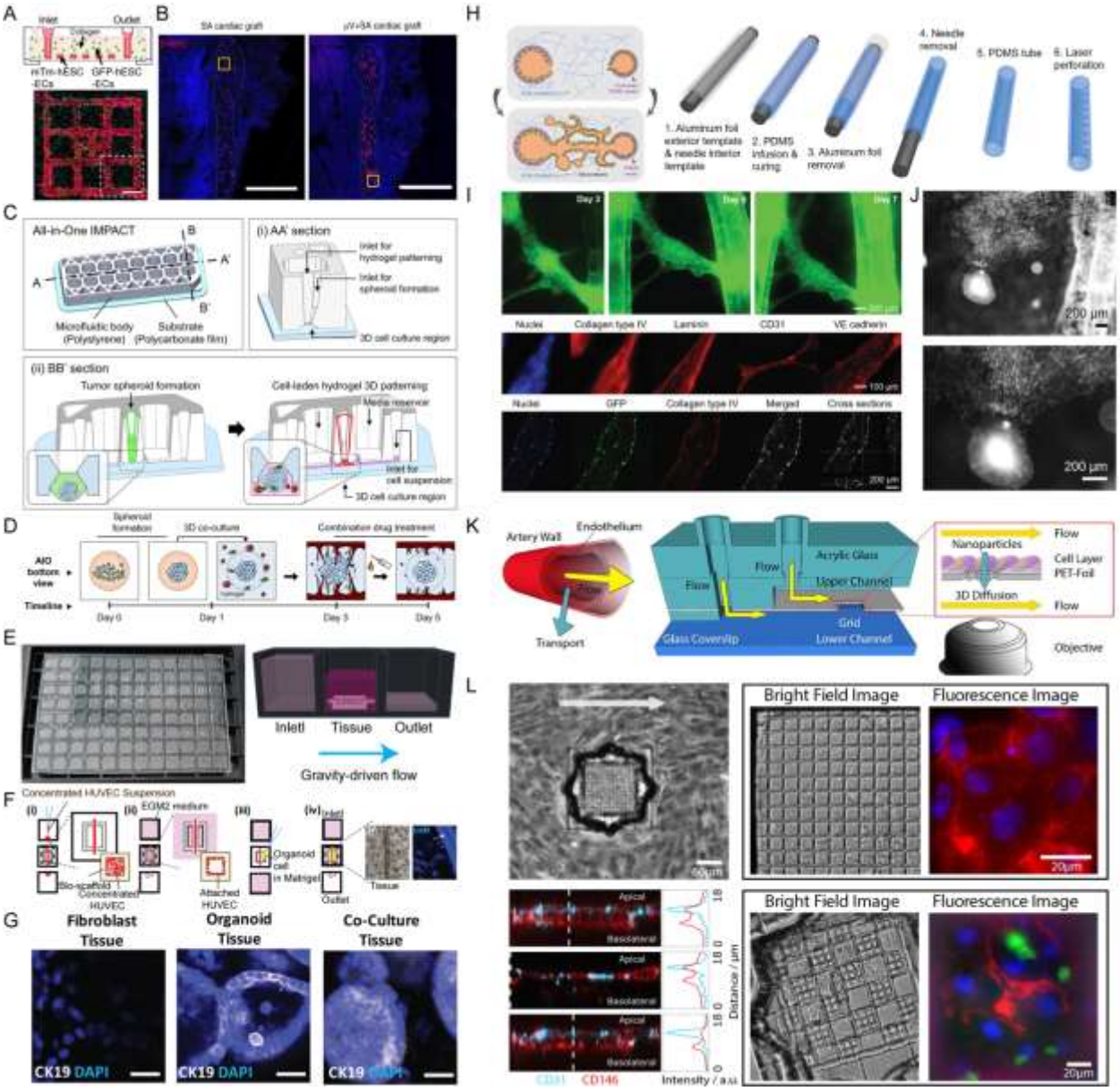

Fig. 2. Microfluidic technologies to mimic tissue vascularization. (A) Schematic of the perfusable constructs utilizing hESC-ECs. The fluorescence imaging below showing DsRed (red) stained mTm-expressing hESC-ECs and GFP (green) stained GFP-expressing hESC-ECs in the patterned network. Scale bar, 500 μm. (B) Infarcted athymic Sprague-Dawley rat hearts were stained with human-specific β-myosin heavy chain (β-MHC, red) to assess graft retention. Scale bar, 1 mm. Reproduced with permission from ref.

171. (C) Schematic showing the All-in-One-IMPACT. (D) Drug screening process on metastatic cancer model using All-in-One-IMPACT. Reproduced with permission from ref. 173. (E) Image of the nighty six-well plate-based and the three-well-based system. Reproduced with permission from ref. 176. (F) Schematic of the fabrication and cell seeding process on the InVADE platform. (G) Confocal image showing the immunostaining of cultured tissues for cytokeratin 19 (CK19, white). Scale bar, 20 μm. Reproduced with permission from ref. 177. (H) Schematics showing the fabrication of perforated PDMS tubes through focused laser ablation and their angiogenesis modeling performance. (I) Fluorescence micrograph of larger vessels formed between two PDMS tubes and expressed endothelial biomarkers. Green fluorescence showing the presence of GFP-labeled HUVECs. (J) Angiogenesis of tumor spheroid with perforated PDMS tubes. Reproduced with permission from ref. 180. (K) Schematics showing the design for high-resolution imaging in the microfluidic system. (L) The observation of cells from the microfluidic device. ECs were stained with Alexa647-conjugated anti-CD31/PECAM-1 antibody (red), and their nuclei were labeled with Hoechst 33342 (blue). Pericytes were stained with Nuclear Green (green). Reproduced with permission from ref. 182.

4. Bioprinting

Bioprinting involves using computer-aided processes to create 3D structures composed of living cells and biomaterials. It has wide-ranging applications in tissue engineering, regenerative medicine, and drug screening.[43] The promise of this technology lies in its ability to craft intricate and functional biological tissues and organs that could be used for transplantation, disease modeling, and drug development.[44] Here, we will begin by introducing the general background about the most studied bioprinting technologies and then proceed to their advancements in tissue vascularization.

4.1 General bioprinting technologies

4.1.1 Inkjet bioprinting

Inkjet bioprinting takes inspiration from conventional paper printing by dispensing tiny bioink droplets onto a membrane surface. This process relies on the interplay between the droplets and the membrane to stabilize the resulting structure.[184] Unlike some alternative methods, inkjet bioprinting stands out due to its minimal impact on cells, facilitated by the gentle propelling forces utilized.[185]

Different mechanisms, such as thermal,[186] piezoelectric,[187] or electrostatic[188] generate droplets in drop-on-demand inkjet bioprinting, allowing for various tissue constructs. Thermal inkjet achieves

ink propulsion by causing localized bioink evaporation, resulting in bubble-formation that creates pressure to propel the bioink through the nozzle.[189] This approach involves brief to extreme heating, which inflicts fewer cell casualties than some other bioprinting methodologies. Remarkably, it maintains high cell viability ratios under suitable conditions, often reaching around 90% survival.[186] Piezoelectric bioprinting harnesses acoustic forces to dispense bioink droplets,[187] while electromagnetic inkjet bioprinting employs magnetic forces to propel the bioink onto the membrane.[190] However, both approaches face limitations related to bioink viscosity requirement, as their propelling forces are relatively modest. Additionally, the challenge of cell fragmentation during bioprinting disrupts the attainment of uniform cell arrangements.[185] Consequently, numerous research groups are actively exploring suitable materials and methodologies to enhance inkjet bioprinting.[191]

4.1.2 Extrusion-based bioprinting

Extrusion-based bioprinting (EBB) stands as a leading technique in 3D bioprinting. EBB is known for its economic viability, high-cell density combability, and adaptability to various hydrogel viscosities.[192] The EBB process typically begins by selecting a suitable hydrogel prepolymer with sufficient yield stress to maintain the intended structure's form before solidification. Subsequently, mechanical or pneumatic forces are employed to extrude cell-laden hydrogels, guided by computer-designed programs, layer by layer. Following the printing process, the model undergoes crosslinking, achieved through physical agents such as calcium ions or chemical agents such as photocrosslinking, to solidify its shape.[193] Despite EBB's popularity, specific challenges remain that must be addressed, such as limited choices of bioink with optimal printability, compromised resolution, and the delicate balance between printing speed and continuity.[194] The selection of biomaterials as bioinks is crucial in EBB. The chosen biomaterials must possess the strength to maintain shape integrity before crosslinking, be compatible with cells, and exhibit optimal viscosity.[195,196] Numerous evaluations of bioink materials have been conducted, such as those based off gelatin[197] and alginate.[198]

Consequently, EBB's prominence primarily thrives in the high-density bioprinting of human tissues.[199] Researchers have successfully demonstrated extrusion bioprinting for kidney organoids (**Fig. 3A**).[200] Their findings highlighted enhanced cell reproducibility, size, and shape-retention, alongside a more intricate and organized structure compared to conventional cultivation techniques (**Fig. 3B**). This underscores the significant potential of EBB in advancing tissue engineering and

regenerative medicine. Moreover, introducing the Freeform Reversible Embedding of Suspended Hydrogels (FRESH) or similar embedded bioprinting techniques has brought about a shift in complex organ bioprinting with the extrusion method.[201] FRESH employs a supportive bath to preserve design integrity during bioprinting, transcending the limitations of conventional layer-by-layer methods and enabling bioink to be the entire 3D space, thereby greatly enhancing printing flexibility.

4.1.3 Light-based vat-polymerization bioprinting

Stereolithography (SLA) remains a commonly used approach among all the vat-photopolymerization methods.[202] In SLA, the liquid bioink undergoes photoactivated solidification through individual laser shots in a rasterized manner. The printing process involves repetitively moving the build platform and curing individual patterns within a resin layer to assemble a solid 3D object. For the post-polymerization, the bioinks are permanently cured through heating or photocuring, also termed crosslinking.[203]

As an alternative to SLA, digital light processing (DLP) presents a more efficient way of utilizing a digital mirror device or a liquid crystal display to project a designed pattern onto the bioink.[204] Since DLP allows the exposure of each layer to light simultaneously, printing efficiency is effectively improved in a direct layer-by-layer manner.[205] DLP can be categorized into top-down and bottom-up by the direction of light projecting.[206] Utilizing light as a trigger to form bonds between molecules, DLP is facilitated by various polymerization methods such as free-radical chain polymerization[207] and thiol-ene photocrosslinking.[208] Photoinitiators are pivotal in initiating solidification, with type I initiators creating free radicals that initiate the polymerization process[209] and type II initiators transforming energy into radical species for crosslinking.[194]

However, DLP shares similar limitations with SLA, revolving around the viscosity and strength of bioink materials.[210] To expedite the printing process while maintaining method stability, a silk fibroin (SF)-based bioink was developed (**Fig. 3C**).[211] SF imparts robust material strength, superior for *in vivo* implantation (**Fig. 3D**). Also notably, DLP bioprinting was effectively employed to create liver microtissues using the decellularized ECM (dECM).[212] This work highlighted the advantageous high resolution of photopolymerized printing in enhancing liver model development.

To overcome geometric constraints and enhance the bioprinting speed, volumetric additive manufacturing (VAM) has gained attention for biomedical applications.[213–215] VAM involves selectively solidifying a photosensitive resin volume using evolving light patterns projected onto

a rotating container, which shows promise for creating complex shapes and structures more efficiently.[63] However, the limited availability of suitable (bio)inks currently hinders the full realization of VAM's potential in various applications. In recent work, we reported volumetric bioprinting with unmodified silk-based bioinks silk sericin (SS) and SF to create intricate shapes and architectures (**Fig. 3E**).[216] Through subsequent processing, SS constructs exhibited reversible shape-memory behavior, while SF constructs showcased adjustable mechanical properties spanning from low-Pa to high-MPa ranges. Both silk bioinks showed excellent cytocompatibility towards C2C12 myoblasts (**Fig. 3F**). With a double-crosslinked network, the VAM-printed 10% SF screws with good mechanical strength could be implanted into a pre-drilled hole within the cortical bone (**Fig. 3G**), suggesting the potential for orthopedic applications.

4.1.4 Laser-assisted bioprinting

For laser-assisted bioprinting (LAB), a combination of a ribbon coated with liquid biomaterials, a pulsed laser source, and a specially prepared substrate is utilized to deposit biomaterials.[217] During this process, lasers operating in the nanosecond range and emitting at UV or near-UV wavelengths are used to illuminate the coated ribbon.[218] This illumination leads to the evaporation of the bio-materials, causing them to form droplets that land on the substrate. This substrate is typically treated with a biopolymer or a medium conducive to cell culture, which aids in the attachment and subsequent growth of cells after their transfer.[219] The precision of LAB is dependent on various factors, including the thickness and rheological features of biomaterials, the energy of the laser pulses, the substrate's capacity to absorb liquids, the speed of printing, and the overall arrangement of the planned structure.[220–222]

Originally developed for precise metal deposition in 1986,[223] laser-induced forward transfer (LIFT) has been excelling in micron-level precision, capable of isolating single cells or clusters from highly concentrated bioink.[224] The high-throughput capacity of LIFT, capable of reaching up to 5 kHz, allows for the rapid printing of thousands of droplets every second.[225] Unique to LIFT is its nozzle-free design, which eliminates clogging problems, a common issue when using viscous bioinks.[226] This technique is also notable for its ability to maintain high cell viability, outperforming other bioprinting methods, and making it particularly effective for in-situ printing.[227] The compatibility of LIFT with other bioprinting technologies further enhances its utility, making it a powerful and adaptable tool in the realm of advanced tissue engineering.[228]

LAB has shown promising in working with various cell types, such as human embryonic stem cell-derived limbal epithelial stem cells (hESC-LESCs) to replicate epithelial structures and human adipose tissue-derived stem cells (hASCs) to create layered constructs resembling the stroma in native corneal tissue.[229] In a different study, the combination of nano-hydroxyapatite (nHA) with mesenchymal stem cells (MSCs) was explored.[230] This research focused on the effects of two different cell-printing shapes, a disc and a ring, showcasing the adaptability of laser-based cell printing in bone repair applications. Additionally, LAB has been instrumental in studying and influencing dynamic matrix remodeling in various fibroblastic populations and structures, particularly in collagen environments.[231]

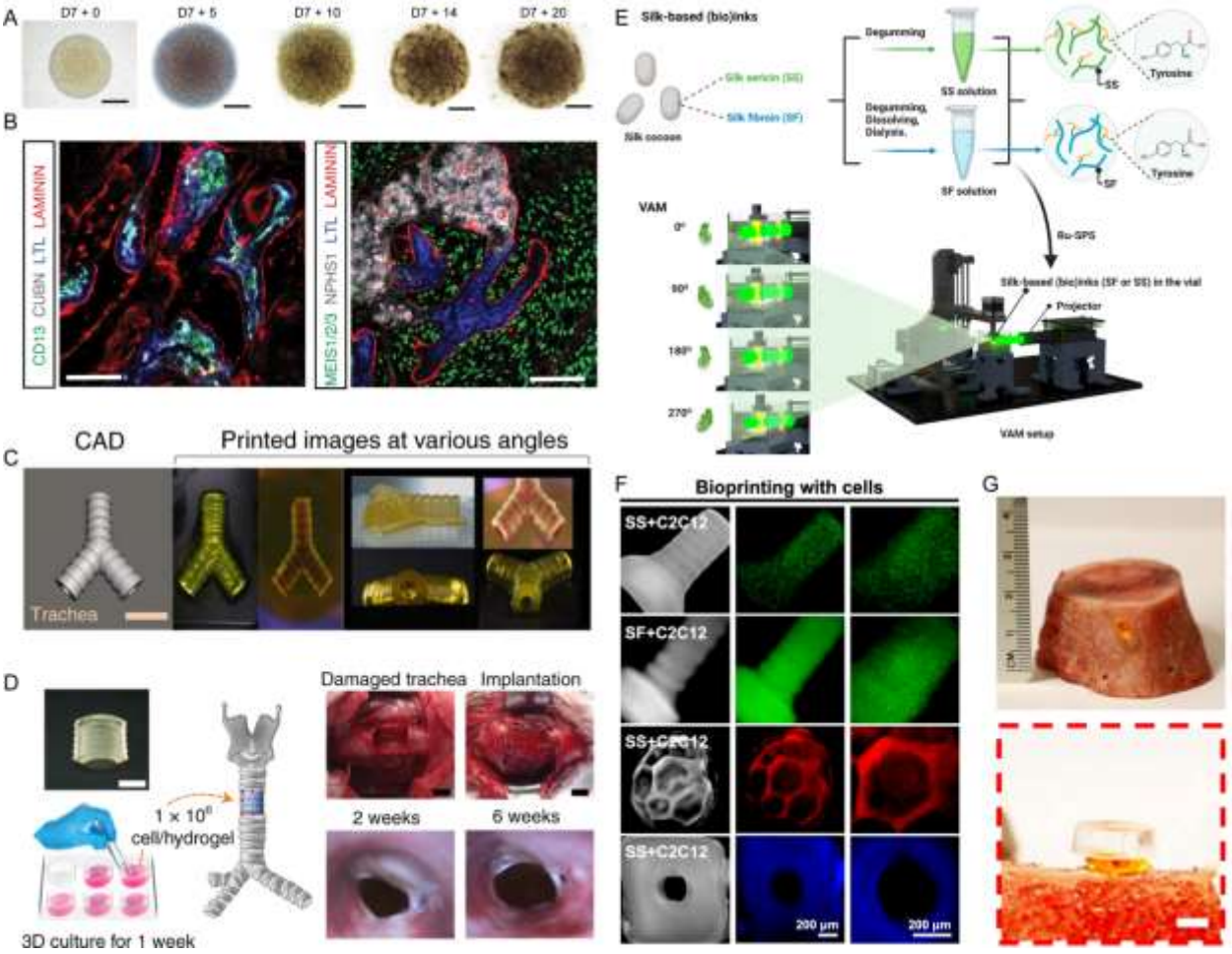

Fig. 3. General bioprinting technologies. (A, B) Extrusion-based 3D cellular bioprinting of (A) kidney organoids and (B) corresponding immunofluorescence showing the presence of proximal tubular segments (CD13 and CUBN), podocytes (NPHS1), proximal tubules (LTL), tubular basement membranes (LAMININ) and surrounding stroma (MEIS1/2/3). Scale bars, 100 µm. Reproduced with permission from

ref. 200. (C) DLP-printed trachea structure using SF-based bioink. Scale bar, 1 cm. (D) Bioprinted Sil-MA trachea laden with chondrocyte for *in vivo* implantation. Scale bars, 5 mm. Reproduced with permission from ref. 211. (E) Schematic of the preparation of silk-based (bio)inks and the setup for VAM. (F) Fluorescence microscopic images of different volumetrically bioprinted C2C12 cell-laden structures with SS or SF. (G) Photograph showing the implantation of a volumetrically printed screw. Scale bar, 1.5 mm. Reproduced with permission from ref. 216.

4.2 Bioprinting technologies for tissue vascularization

4.2.1 Inkjet bioprinting

Inkjet bioprinting has favored vascularization due to significant merits, such as precise droplet size and deposition controllability, easy scale-up, and high printing speed and resolution.[184] Electrohydrodynamic (EHD) inkjet bioprinting has recently been developed to fabricate hydrogel-based microvascular tissues containing intricate hierarchical and branching channels. The method achieved a minimum feature size of 30 μm, closely approximating the size of natural capillary blood vessels (**Fig. 4A**).[232] Inkjet bioprinting has also been used for sacrificial template printing. In one study, authors successfully employed gellan gum as a sacrificial material to fabricate complex vascular networks using 3D inkjet printing within 3D-gelatin gels. They further demonstrated the perfusion of human whole blood through these vascular tubes at a flow rate of 3.0 cm s^{-1} for 2 hours (**Fig. 4B**).[233]

4.2.2 EBB

EBB involves depositing cell-laden bioinks layer by layer, enabling the creation of tissue structures with integrated vascular networks. The main strength of EBB lies in its versatility to incorporate various materials and cell types, facilitating the fabrication of complex and functional vascular systems necessary for tissue viability. By combining endothelial cells, fibroblasts, and adipose tissue-derived MSCs, researchers have created spheroids that promote vascular outgrowth and integration with host vasculature.[234] Optimizing photocrosslinking conditions ensures the stability and viability of these constructs, supporting the development of functional microvascular networks. To fabricate complex and functional vascular systems, sheet-based extrusion bioprinting with GelMA hydrogels represents a substantial advancement.[235] By utilizing endothelial cells and pericytes, sheet-based extrusion bioprinting enabled microvascular construction. EBB can be further utilized to fabricate vascularized tissues. Microgel-based biphasic (MB) bioink was developed to generate cardiac tissues and organoids when encapsulating human-induced

pluripotent stem cells, facilitating stem cell proliferation and cardiac differentiation.[236] Additionally, hepatic metastasis models of various cancer types were fabricated with sacrificial-free direct ink writing (SF-DIW) approach, providing a platform to investigate the cytostatic activity of anti-cancer drugs.[237]

4.2.3 Light-based vat-polymerization bioprinting

4.2.3.1 SLA bioprinting

SLA bioprinting, particularly using dynamic optical projection stereolithography (DOPS), offers precise control and high resolution, making it suitable for creating complex vascular networks.[238] By optimizing parameters such as UV intensity, exposure time, and cell density, SLA bioprinting can produce different structures with high cell viability. Complex cell-encapsulated structures, such as 3D Y-shaped tubular constructs, can be printed through SLA.[239] With optimized parameters, such as cure depth, a cell viability of 75% was achieved immediately after printing within the Y-shaped structure. In addition to the shape, size is also crucial for mimicking real tissue. A fast SLA printing method was developed to create large-scale biocompatible hydrogel models with embedded vascular networks, which supported cells with high viability and function.[240] These studies together underscore the potential of SLA bioprinting in advancing tissue engineering and regenerative medicine by optimizing bioink composition and printing parameters to achieve desired structural and functional outcomes.

4.2.3.2 DLP bioprinting

DLP is a promising avenue for crafting volumetric scaffolds endowed with perfusable vascular channels.[241] The productive utilization of DLP bioprinting requires the employment of appropriate low-viscosity photo-reactive bioinks, which can be solidified using cytocompatible light sources, either longer wavelength UV light (365 nm) or visible light (400–700 nm).[205] Therefore, current research is primarily centered around developing innovative bioink formulations.[242–244] Decellularized ECM sourced from organs and tissues is particularly valued for its inherent biochemical signals, which can support and expedite processes of repair and regrowth within the body.[245] A new bioink termed methacrylated bone-derived biomaterial (BoneMA), made from methacrylate-modified human bone-derived ECM, has been developed (**Fig. 4C**).[246] This hydrogel possessed tunable mechanical properties and maintained nanoscale features of polymer networks, which was highly compatible with cells and supported the formation of interconnected vascular networks.

Although methacrylated polymers have been commonly used for DLP printing, the high concentrations of propagating radicals produced during crosslinking could damage sensitive cell types.[207] In addition, the high crosslinking density of DLP-bioprinted hydrogels leads to a decrease in the viability of the enclosed cells.[39] The emergence of norbornene-based bioinks has been a promising alternative to methacrylated macromers in 3D bioprinting. Recently, gelatin-norbornene (GelNB) was reported for DLP bioprinting (**Fig. 4D**).[247] Formulated at low concentrations (2–5 wt.%), a wide range of stiffness levels can be achieved. Notably, the GelNB hydrogels demonstrated high cytocompatibility, as evident from the favorable viability of encapsulated HUVECs, which also formed a well-connected microvascular network (**Fig. 4E**).

4.2.3 LAB

Due to its accuracy and efficiency, LAB has emerged as a highly versatile technology for the precise deposition of minute substances.[218] LAB is commonly used to develop microvascular networks in a specific pattern, which can be maintained while introducing an additional layer of endothelial cells on the surface.[248] LAB also addresses the limitations of other bioprinting methods by avoiding issues such as clogging and enabling high-resolution bioprinting of high-density cell droplets, which makes it suitable for creating endothelial capillary patterns and constructing complex vascular structures.[249] For example, LAB was used to arrange endothelial cells with MSCs into patterns with high density, enabling the creation of a vascular network with a predetermined architecture (**Fig. 4F**).[250] This further facilitates the application of LAB for *in vitro* prevascularization of certain organs, such as bone.[135] Human osseous cells were confirmed to create prevascularized constructs through LAB for autologous bone reparation (**Fig. 4G**),[251] providing a promising method for addressing the challenge of cell viability within voluminous bone tissues. Notably, LAB's effectiveness in promoting bone regeneration has also been proven *in vivo* in this work.

5. Microfluidics-assisted bioprinting for tissue vascularization

5.1 Limitation of microfluidic and bioprinting technologies for tissue vascularization

Microfluidic technologies excel in microscale fluid flow control, effectively mimicking the behavior of blood vessels on a smaller scale.[139,140] However, integrating these technologies into larger, more complex tissue structures poses significant challenges.[55] As channels expand from microscopic to millimeter sizes, difficulties arise in managing the geometry, diameter, and layering

of the replicated vessels.[252] Another issue is the limited throughput of microfluidic devices.[253] Techniques such as mold casting, offers insufficient control over vessel size and cell placement, which hampers sustained cell viability in thicker tissues.[254] Scaling microfluidic models to larger tissue constructs introduces additional complexities, particularly in maintaining a physiological environment that supports cell health and tissue functionality.[255] Ensuring consistent perfusion and oxygenation is crucial, yet replicating the detailed vascular networks found in natural tissues is extremely challenging.[256] Additionally, there is a continuous struggle with material compatibility in microfluidic fabrication, underscoring the need for the development of biocompatible materials that can both resemble the natural ECM and enhance vascularization within these systems.[257]

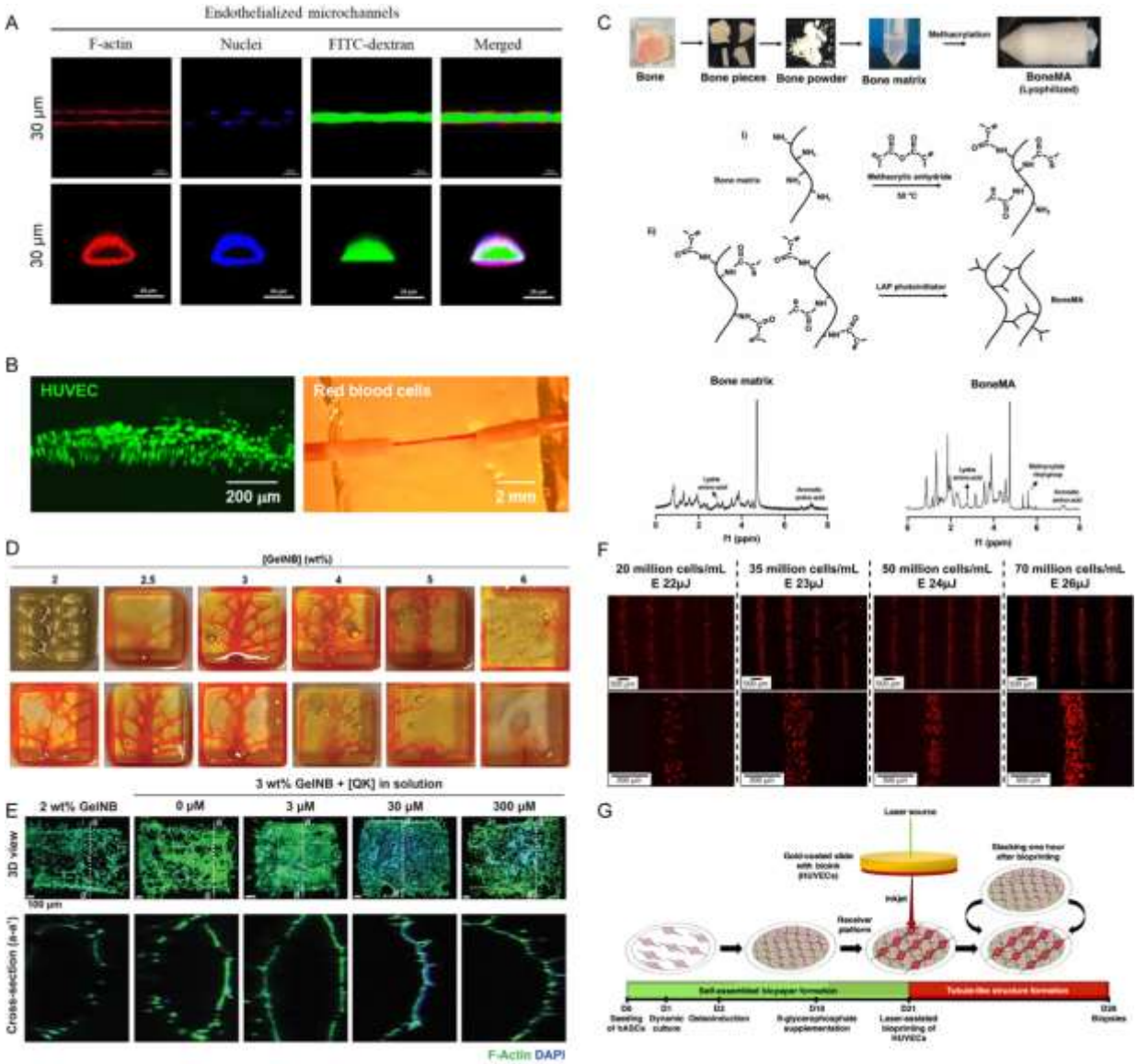

Fig. 4. Conventional bioprinting technologies for tissue vascularization. (A) Fluorescence images showing the flow perfusion within the channel of microvascular networks fabricated through EHD inkjet printing. Reproduced with permission from ref. 232. (B) Images of inkjet-printed vasculature with HUVEC and the flow behavior with blood. Reproduced with permission from ref. 233. (C) Schematics representation of the synthesis and chemistry of BoneMA for DLP bioprinting. Reproduced with permission from ref. 246. (D) Images showing the pattern constructed by DLP printing with different concentrations of GelNB. (E) Confocal microscopy images showing 3D views and cross-sections of HUVEC-seeded channels. Reproduced with permission from ref. 247. (F) Fluorescence images showing capillary-like network bioprinted with different cell density and laser energies. Reproduced with permission from ref. 250. (G) Schematic showing the preparation of biopaper and LAB process. Reproduced with permission from ref. 251.

Bioprinting has made remarkable progress but continues to face the substantial challenge of accurately mimicking the complex, multi-scale structure of natural blood vessels in 3D tissue models.[258] A key limitation is the inability to replicate the exact sizes and tubular structures of native tissue vessels.[259] In particular, current EBB methods struggle with resolution, especially for objects smaller than 100–200 μm, complicating the process of achieving effective tissue microvascularization.[260] Furthermore, while LAB offers better resolution, it is hindered by high costs and difficulties in bioprinting multiple materials at once.[261] The complex, hierarchical arrangement of natural vascular networks, which includes arteries, veins, and capillaries, also poses a significant challenge.[262] Overcoming these issues requires a collaborative, interdisciplinary approach to further enhance the capacities of bioprinting technologies.

5.2 The integration of microfluidic and bioprinting technologies

The combination of bioprinting with microfluidic technologies presents a promising solution to the complex challenge of tissue vascularization.[40] This integrated approach aims to synergistically overcome the individual limitations of each technology.[263,264] By incorporating microfluidic technologies into bioprinters, the fabrication of more precise channels becomes possible.[265] These channels are designed to mimic the complex branching and perfusion required for effective nutrient and oxygen distribution, addressing key issues of perfusion and oxygenation in bioprinted tissues.[266] This cooperative strategy capitalizes on the precise cell and biomaterial-deposition capabilities of bioprinting, combined with the microscale control inherent in microfluidics.[267] This convergence is paving the way towards more lifelike and clinically relevant tissue models with

enhanced vascularization. The fusion of bioprinting and microfluidics is a significant stride in tissue engineering, aiming to produce robust, perfusable, and physiologically functional tissues suitable for regenerative medicine applications.[268,269] In this section, we will focus on the recent developments in microfluidic assisted extrusion (microfluidic coaxial bioprinting) and DLP bioprinting for tissue vascularization.

5.2.1 Microfluidic inkjet bioprinting

Combining microfluidics with inkjet bioprinting merges the precise control of fluid dynamics in microfluidic systems with the high-resolution patterning capabilities of inkjet printing. This integration may facilitate real-time switching and mixing of different bioinks, which is crucial for improving the resolution and structural integrity of bioprinted tissues. Microfluidic inkjet bioprinting offers the potential to create highly accurate and reproducible human tissue and organ models, significantly improving pharmaceutical testing. For example, cellular interactions can be enhanced by building micrometer-sized multilayers between cells and proteins through microfluidic inkjet bioprinting, which is crucial for 3D human tissue chip fabrication and further drug evaluations.[270] Moreover, cell-cell interactions between different cells, such as HepG2 liver cells and U251 cancer cells, were improved through precise microscale cell patterning on microfluidic chips using microfluidic inkjet bioprinting.[271] With the understanding of these basic functions, liver-on-a-chip models were developed and essential liver functions and interactions can be replicated, enabling sophisticated disease modeling and drug toxicity assessments.[272]

5.2.2 Microfluidic extrusion bioprinting

5.2.2.1 Microfluidic coaxial bioprinting

Extrusion-based 3D bioprinting plays a critical role in tissue engineering, enabling the creation of structures that closely resemble real tissues.[273] However, there is a need to improve the resolution and intricacy of the produced structures, indicating the necessity for ongoing advancements. A significant development in this area is the integration of microfluidic systems into extrusion bioprinters, termed microfluidic coaxial bioprinting.[274] This innovation marks a significant step forward, providing precise control over bioink volumes and enabling the simultaneous extrusion of multiple bioinks through a single nozzle.[275] Various groups have successfully achieved the fabrication of vessels with diverse thicknesses, scales, and intricate shapes by manipulating the number of nozzles, adjusting material viscosity, and fine-tuning crosslinking parameters.[276,277]

GelMA is commonly used to construct blood vessel-like structures.[120] A digitally coded coaxial extrusion device was developed by us, which allowed for the continuous fabrication of complex 3D tubular hollow fibers with multiple circumferential layers in a single step (**Fig. 5A**).[278] By incorporating human smooth muscle cells (hSMCs) and HUVECs in the bioinks, the bioprinted tissues demonstrated cellular heterogeneity and phenotypes similar to the natural blood vessel (**Fig. 5B**). Their ability to be actively perfused with fluids and nutrients was confirmed as well (**Fig. 5C**), which holds potential in a wide range of medical and biological applications.

Although these bioprinted vascular conduits have been shown to mimic the structural of native blood vessels, they generally displayed significantly lower mechanical strength compared to natural vessels, which limited their use in biological applications that require a physiological setting.[279] Thus, the challenge persists in bioprinting vascular conduits that are not only structurally comparable but also match the mechanical and functional properties of small-diameter native vascular grafts. Recently, we developed a robust double-network (DN) hydrogel (bio)ink, where energy-dissipating ionically crosslinked alginate and elastic enzyme-crosslinked gelatin were included to provide mechanical properties and functionality (**Fig. 5D**).[280] Both single- and dual-layered hollow conduits were fabricated to mimic vein-like and artery-like tissues (**Fig. 5E**). The vascular functionality was similar to physiological vasoconstriction and vasodilation responses. In addition, the potential of these bioprinted conduits for clinical applications was investigated, including the susceptibility to pseudo-viral infection from the severe acute respiratory syndrome coronavirus 2 (SARS-CoV-2) (**Fig. 5F**).

However, coaxial bioprinting still has room for refinement. Challenges such as approaching diameter limitations, advancing basic biological techniques, and shortening printing times without compromising sensitive cells must be addressed for further progress.[281,282] To enhance the resolution of printed structure, we developed a strategy utilizing post-printing treatment, termed shrinking printing.[283] Based on charge compensation, the shrinking effect occurs when placing hyaluronic acid methacrylate (HAMA) hydrogel within high charge density polycations, which leads to the expulsion of water and size reduction (**Fig. 5G**). While bioprinted with cells, good biocompatibility and proliferation were observed after shrinking (**Fig. 5H**). In another research, we developed a method focused on crafting standalone cannular tissues with extremely small luminal diameters and very thin walls.[284] This method employed an aqueous two-phase system, integrating both embedded bioprinting and cutting-edge crosslinking and extrusion techniques,

which enabled precise deposition of aqueous bioinks, such as GelMA, within a stable non-mixing aqueous support bath composed of poly(ethylene oxide) (**Fig. 5I**). As a result, we successfully created standalone hollow structures with diameters around 40 μm and walls thinner than 5 μm (**Fig. 5J)**. The technique also maintained cellular functionality, proving its adaptability and effectiveness (**Fig. 5K**). This innovation is particularly promising for its applications in regenerative medicine and in crafting complex tissue models.

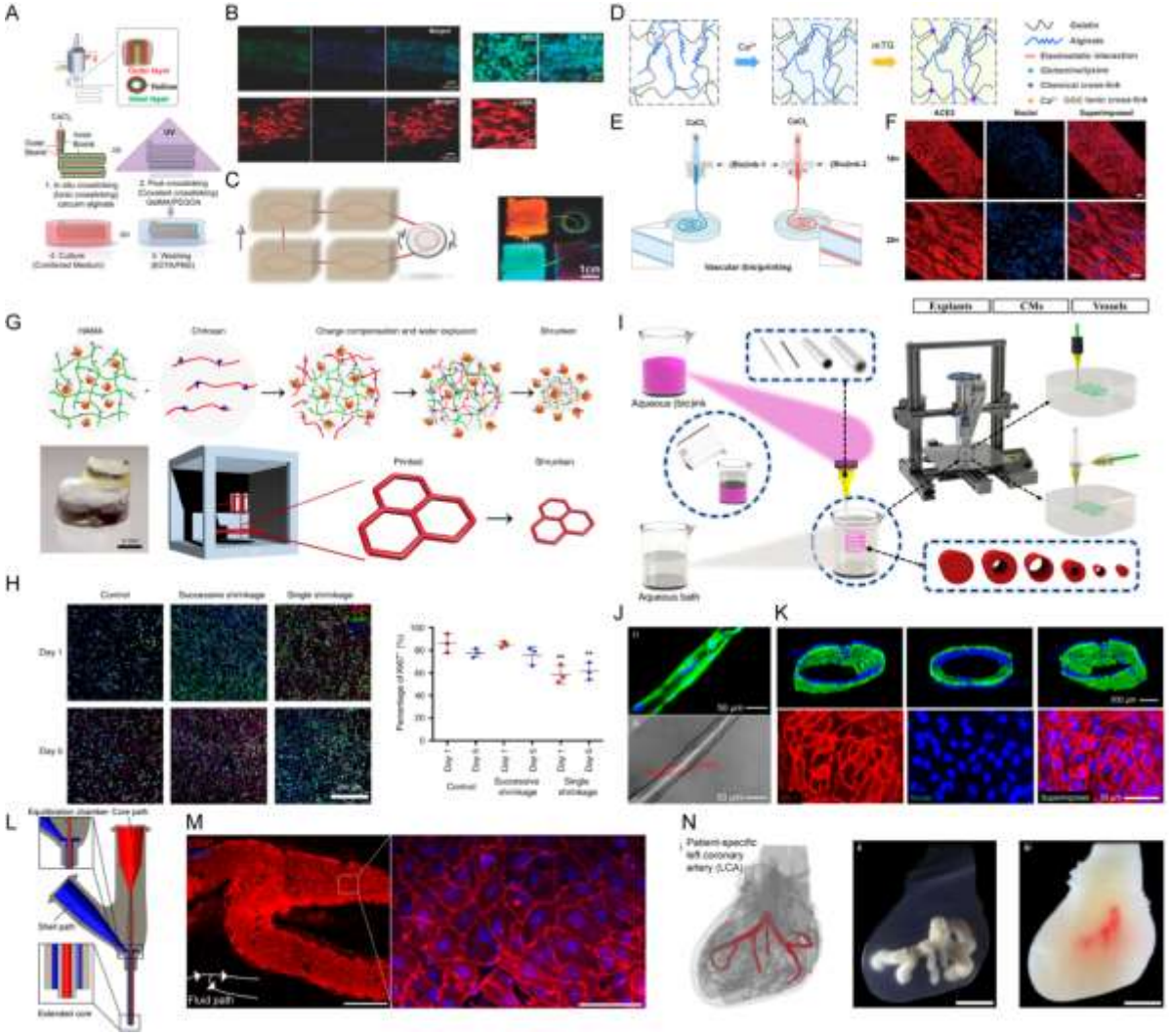

Fig. 5. Microfluidic coaxial bioprinting for tissue vascularization. (A) Schematic showing the bioprinting of multilayered hollow structure. (B) Immunostaining of bioprinted vascular tubes with vascular biomarkers for HUVECs (CD31, green) and hSMCs (α-SMA, red). Nuclei were labeled with DAPI (blue). (C) Schematic and images of the perfusion through multiple tissues. Reproduced with permission from ref. 278. (D) Schematic showing the crosslinking mechanism of the DN bioink. (E) Schematic representation

of the bioprinting process for monolayered and dual-layered vascular conduits. (F) Fluorescence photography showing the expression of ACE2 (red) within bioprinted vascular conduits. Scale bars, 100 μm. Reproduced with permission from ref. 280. (G) Schematic showing the shrinking process and corresponding size reduction. (H) Fluorescence images showing the immunostaining of MCF-7 cells with cell proliferation marker Ki67 (red). MCF-7 cells were stained for F-actin (green) and nuclei were labeled with DAPI (blue). Reproduced with permission from ref. 283. (I) Schematic illustration of the two-phase aqueous embedded (bio)printing strategy. (J) Wall thickness and diameter of a coaxially printed cannular tissue, stained for F-actin (green). Nuclei were labeled with DAPI (blue). (K) Fluorescence micrographs of the HUVECs-seeded vascular conduits (stained for F-actin, green) and the expression of ZO-1 (red). Nuclei were labeled with DAPI (blue). Reproduced with permission from ref. 284. (L) Illustration of the extended printhead with core-shell design. (M) Confocal image of endothelial cells arranged within a bioprinted blood vessel. Scale bar, 1 mm. Cells were stained with CD31 (red) and nuclei were labeled with DAPI (blue). Scale bar, 50 μm. (N) From left to right: CAD rendering of printed LCA structure, printed LCA in alginate microparticles and the completed patient specific LCA. Scale bar, 5 mm. Reproduced with permission from ref. 285.

Despite advancements in creating perfusable channels, coaxial bioprinting still falls short in replicating the complex branching and multilayer architecture of native vessels. To tackle this challenge, researchers developed two innovative methods to fabricate branching vascular networks within soft materials: coaxial embedded printing (co-EMB3DP) and coaxial sacrificial writing into functional tissues (co-SWIFT).[285] Both techniques employ a core-shell printhead with an extended core channel (**Fig. 5L**). The branch points were created by using the extended core nozzle to puncture the shell wall of existing filaments, followed by coaxial extrusion of core and shell inks to ensure proper connections. By repeating the punching and reconnecting, complex branching vascular networks were fabricated. To enhance the physiological accuracy, branched vessels were bioprinted with co-EMB3DP, where smooth muscle cells (SMCs) were included in the shell bioink, and sacrificial gelatin was used as the core ink. After seeding endothelial cells, a continuous monolayer on the inner surfaces of the vessels could be observed (**Fig. 5M**). To further demonstrate the capability of co-SWIFT for personalized biomanufacturing, a patient-specific left coronary artery (LCA) was printed within a transparent alginate matrix (**Fig. 5N**). This work shows possibilities for scalable biomanufacturing of branching vascularized tissues in disease modeling and drug screening.

5.2.2.2 Pre-set EBB

To address the limitations in replicating the complex structure of native tissues, pre-set EBB was developed, which can create heterogeneous, multicellular, and multimaterial structures simultaneously.[286] The key notion of this method was the use of a precursor cartridge to maintain the configuration between different materials, which can then be bioprinted through a syringe-based printhead. The introduction of the precursor cartridge allows precise deposition of multiple materials into complex structures without compromising cell viability. Using this system, real tissue-like structures such as spinal cords, blood vessels, and capillaries were successfully fabricated. In addition, multiscale hepatic lobules within a highly vascularized construct were fabricated by pre-set EBB.[287] Bioprinted with HepG2 and endothelial cells, these hepatic lobules demonstrated higher enzyme activity compared to homogeneous cell bioprinting, highlighting the potential of pre-set EBB for creating functional tissues with high fidelity.

5.2.3. Microfluidics-assisted DLP bioprinting

Human organs, including veins and arteries, exhibit multiscale, hierarchical structures, particularly at bifurcation points.[4] Despite advancements in DLP bioprinting, significant hurdles persist. These include the challenge of precisely bioprinting complex, multicomponent tissue constructs that mimic these natural structures, and the difficulty in managing material contamination during transitions between different printing materials.[43] These obstacles highlight the need for further refinement in DLP bioprinting techniques to accurately replicate the intricate designs found in human tissues.

A primary issue is managing material contamination during transitions between different bioinks.[288] Our group has pioneered a method that incorporates a microfluidic device into a digital micromirror device (DMD)-based bioprinter, enabling the creation of multimaterial constructs through stereolithographic bioprinting.[289] This system included a UV lamp at 385 nm, various optical lenses and objectives, a DMD chip, and a microfluidic device (**Fig. 6A**). We evaluated the multimaterial capabilities of this bioprinting setup through an *in vivo* angiogenesis study using a rat subcutaneous implantation model. The *in vivo* experiment involved constructing a four-material framework, utilizing poly(ethylene glycol)-diacrylate (PEGDA) for the structure, and embedding three GelMA strips infused with vascular endothelial growth factor (VEGF). The incorporation of VEGF in these multimaterial constructs resulted in increased blood vessel formation within the implants (**Fig. 6B**) and heightened CD31 expression in the infiltrating cells (**Fig. 6C**). This *in vivo*

experiment underscored our ability to produce heterogeneous constructs with this microfluidic assisted bioprinting approach, effectively influencing key biological functions like angiogenesis.

While our previous platform allowed rapid material switching, it was limited to discrete gradient material distributions. To enhance this, we proposed a gradient bioprinting system, which combined a DLP 3D bioprinter with a microfluidic mixing chip, specifically designed to produce composable and graded (bio)inks (**Fig. 6D**).[290] This technology enabled us to produce structures with continually or continuously gradient variations, such as a two-dimensional maple leaf, ensuring continuity in specified areas (**Fig. 6E**). We utilized green fluorescent protein-HUVECs (GFP-HUVECs) to bioprint a vascular-like network with the smallest vessels measuring 50 μm in diameter (**Fig. 6F**). The observed imagery revealed a gradient in cellular fluorescence, which was supported by quantitative measurements showing a notable decline in intensity. Moreover, our system facilitated the bioprinting of multiple cell types simultaneously, including GFP-HUVECs and red fluorescent protein-HUVECs (RFP-HUVECs), to create various cell gradients. In addition to material gradients, our system also worked with chemical gradients. For instance, we incorporated a gradient of soluble VEGF (ranging from 0 to 100 ng mL^{-1}) into a heparin methacryloyl-gelatin methacryloyl (HepMA-GelMA) hydrogel matrix. This gradient effectively promoted vessel branching in angiogenesis and vasculogenesis processes. By the 14^{th} day of embryonic development, it was evident that areas with higher VEGF concentrations in the hydrogel exhibited increased growth in both the length and number of blood vessels (**Fig. 6G**), demonstrating the successful implementation of a growth factor gradient and its significant impact on enhancing vascularization. This highlighted the system's immense potential as an effective instrument in the field of tissue regeneration.

In addition to creating structure with multiple materials,[291,292] the integration of DLP bioprinting with microfluidic devices shows significant advances in streamlined operations, facilitating cell culture process to maintain good cell behavior. For example, researchers developed a variable height micromixer (VHM) (**Fig. 6H**), showing improved mixing efficiency at lower flow rates compared to traditional planar designs.[293] With this system, complex cell-laden 3D microstructures were directly bioprinted inside microfluidic channels (**Fig. 6I**). To enhance cell proliferation after printing, we created size-tunable porous structures using a combination of DLP and a microfluidic bubble-generating chip (**Fig. 6J**).[294] The size of the bubbles was precisely controlled within a GelMA hydrogel matrix, producing consistent and reproducible porosities (**Fig. 6K**). High cell

viability of NIH/3T3 fibroblasts was observed after cultivation within the printed porous constructs, demonstrating good cytocompatibility of the printed porous structures and the ability to enable proper cell behaviors (**Fig. 6L**).

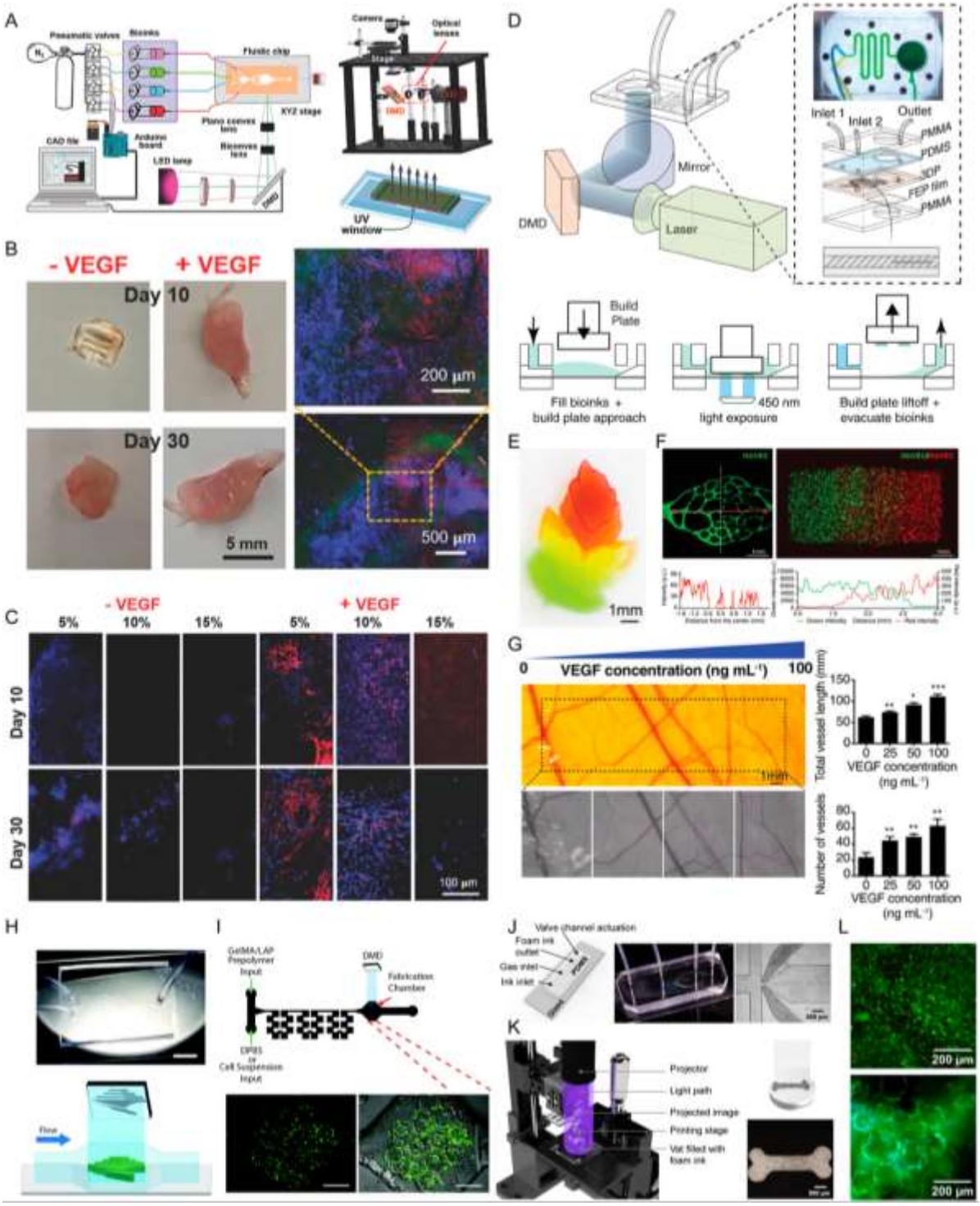

Fig 6. Microfluidic assisted DLP bioprinting for tissue vascularization. (A) Schematics detail the complete setup of the bioprinter, including the optical platform and the microfluidic device. (B) Photographs of the retrieved constructs and corresponding confocal images stained to highlight nuclei (blue) and CD31 (red), with bright-field views given a green pseudocolor. (C) The retrieved implants were stained for CD31 (red) to show the angiogenesis performance with or without VEGF. Nuclei were labeled with DAPI (blue). Reproduced with permission from ref. 289. (D) Illustrations and descriptions outline the setup and workflow of the composable-gradient DLP bioprinting platform. (E) Images of a pseudo-3D maple leaf printed with horizontal gradients, using colors that dynamically shift from green to red during the printing process. (F) A printed vascular network structure showing a horizontal gradient in GFP-HUVECs cell density, and an additional construct features RFP-HUVECs (red) and GFP-HUVECs (green), demonstrating a positive gradient of red cells and a negative gradient of green cells from left to right. (G) Images of the printed construct and the adjacent chorioallantoic membrane (CAM) areas indicate the formation of new microvessels growing toward the implanted hydrogel. Reproduced with permission from ref. 290. (H) Image of the fabricated variable-height micromixer. Scale bar, 5 mm. The illustration below shows the in-device printing process. (I) Top: Illustration showing mixed GelMA/LAP and 10T1/2 cell solution exposed to a digital mask. Bottom: fluorescence (green) and composite images of the bioprinted biomimetic hepatic lobule structure. Scale bars, 5 mm. Reproduced with permission from ref. 293. (J) Left: illustration of the valve-based flow-focusing (vFF) chip for bubble generation. Right: images of the chip and the microfluidic channels. (K) Left: illustration of the DLP top-down 3D printer. Right: schematic of a bone-like structure on the printing stage (top) and an actual printed structure (bottom). (L) Live (green)/dead (red) staining (top) and F-actin filaments (green)/nuclei (blue) staining (bottom) of NIH/3T3 fibroblasts within porous constructs after 14 days. Reproduced with permission from ref. 294.

6. Outlook

Integrating microfluidic systems and bioprinting technologies to create vascular networks for tissue engineering brings forth many promises, offering the potential to overcome a critical barrier in creating functional and viable tissue constructs.[74] Strategies to enhance vascularization in bioprinted constructs may involve incorporating microfluidic channels to support efficient perfusion.[284] Similarly, combining the high-throughput capabilities of microfluidics with the precision of bioprinting has potential for creating complex yet functional vascular networks.[289,290] These innovations facilitate the creation of complex, physiologically relevant structures and have profound implications reverse engineering biological processes, disease modeling, and performing

drug screening for personalized medicine. These models will reduce reliance on animal models and expediting the drug development process.

Moreover, integrating microfluidic technologies in 3D bioprinting significantly enhances the precision and customization of bioinks to create more complex tissue structures. This advancement potentially facilitates improved transplantation outcomes by enabling the creation of vascular structures and providing cell-friendly environments, thus enhancing tissue viability and integration. Bioprinted tissues with personalized properties can be tailored to meet specific clinical needs, reducing immune-rejection risks and promoting faster healing. Additionally, these integrations may allow on-demand tissue production, minimizing the process of tissue transplant, and supporting patient-specific drug testing and development. It is further envisioned that such an approach will ensure more effective, customized therapies with minimized surgical risks, which shows the potential to revolutionize patient care.

Despite the tremendous potential, there are several challenges to be addressed. One primary concern is the long-term stability and functionality of the engineered vasculatures. Ensuring proper perfusion and preventing occlusion within the channels remain critical hurdles, as inadequate circulation can lead to cellular hypoxia and necrosis. In addition, recreating the barrier function of brain vasculature will be important for modeling of brain vascular disorders in malignancies and degenerative brain disorders. To address this issue, there are two aspects to consider: material design and cell fate control. Materials play a crucial role in determining constructed vasculature stability within fabricated scaffolds. The ideal material should closely mimic the properties of ECM, which possess both mechanical strengths to maintain structural and high biocompatibility to allow cells to grow and differentiate.[33,295] While the material only functions as a substrate, the better solution lies in controlling cell growth and differentiation to form engineered vascular in *ex vivo* conditions.[194] Bioprinting offers the advantage of precise arrangement of cells within biomaterials,[197] integrating these technologies with microfluidic systems while maintaining compatibility and mechanical integrity can be complex but promising.

Scaling up while retaining the fidelity of the models for the pathology being modeled presents another challenge. Scaling encompasses both quantity and complexity. To increase quantity, more automated equipment and programmatic experimental design are demanded. Complexity-elevation is a substantial task because of the highly integrated human body, even at an organ or tissue level, where their structural and functional integrity is significant and beyond our

understanding.[6,10] Although microfluidic technology can potentially mimic precious structures, it is still far from faithfully simulating certain kinds of tissue. More importantly, this is a tissue engineering challenge and calls for a deeper understanding of biology. Only after comprehending how the biological system functions, can we effectively replicate it with engineering methods.

The convergence of microfluidic and bioprinting technologies is expected to grow, with investigations focusing on refining hybrid approaches that combine the benefits of both techniques. Exploring additional combinations of microfluidics with 3D bioprinting could expand the potential for developing innovative biomedical applications. For instance, instead of using different materials, bioprinting with various cell types to mimic real tissue functions can introduce significant complexity, which yet presents new opportunities for creating highly functional and physiologically relevant tissue models. Advances in biofabrication techniques, such as high-resolution bioprinting,[296] offer the potential to accurately replicate the intricate architecture of native tissues. Despite these potential benefits, current challenges include ensuring the precise placement and maintenance of multiple cell types within a single construct and achieving the appropriate cellular interactions and signaling required for functional tissue development. Utilizing microfluidic technologies to deliver and position cells directly without the need for scaffolds offers significant opportunities for creating more natural tissue structures. This approach can potentially eliminate the immune response and foreign body reactions associated with scaffolding materials. However, scaffold-free bioprinting remains challenging. One major issue is maintaining the structural integrity and mechanical stability of the bioprinted tissues without the support of scaffolds. Additionally, ensuring homogeneous cell distribution and viability during the bioprinting process is crucial. Innovations in microfluidic technology with enhanced cell-handling techniques should pave the way for future scaffold-free bioprinting methods, potentially leading to breakthroughs in tissue engineering and organ regeneration.

In conclusion, microfluidic and bioprinting technologies represent a pivotal advancement in tissue engineering, offering the prospect of creating vascularized tissue constructs with unprecedented precision and functionality. While challenges exist, the potential impact on biomedicine and tissue engineering is undeniable. With continuous innovation and collaboration, the field is poised to transform the landscape of healthcare and biotechnology, bringing us closer to the reality of laboratory-grown tissues and organs for clinical and preclinical applications.

Conflicts of interest

YSZ consulted for Allevi by 3D Systems, and sits on the scientific advisory board and holds options of Xellar, neither of which however, participated in or biased the work. The other authors declare that they have no known competing financial interests or personal relationships that could have appeared to influence the work reported in this paper.

Acknowledgements

The work is supported by the National Institutes of Health (R21EB025270, R21EB030257, UH3TR003274, R01HL153857, R01HL165176, R01HL166522, R01CA282451, R56EB034702), the National Science Foundation (CBET-EBMS-1936105, CISE-IIS-2225698), Chan-Zuckerberg Initiative (2022-316712), National Institute on Aging and Department of Veterans Affairs (IK2CX002180), and the Brigham Research Institute.

Reference

1 G. L. Koons, M. Diba and A. G. Mikos, *Nat. Rev. Mater.*, 2020, **5**, 584–603.

2 M. N. Hirt, A. Hansen and T. Eschenhagen, *Circ. Res.*, 2014, **114**, 354–367.

3 A. Khademhosseini, R. Langer, J. Borenstein and J. P. Vacanti, *Proc. Natl. Acad. Sci.*, 2006, **103**, 2480–2487.

4 A. Khademhosseini, J. P. Vacanti and R. Langer, *Sci. Am.*, 2009, **300**, 64–71.

5 E. S. Place, N. D. Evans and M. M. Stevens, *Nat. Mater.*, 2009, **8**, 457–470.

6 P. Bianco and P. G. Robey, *Nature*, 2001, **414**, 118–121.

7 L. G. Griffith and G. Naughton, *Science*, 2002, **295**, 1009–1014.

8 S. Yin, W. Zhang, Z. Zhang and X. Jiang, *Adv. Healthc. Mater.*, 2019, **8**, 1801433.

9 J. Rouwkema and A. Khademhosseini, *Trends Biotechnol.*, 2016, **34**, 733–745.

10 E. C. Novosel, C. Kleinhans and P. J. Kluger, *Adv. Drug Deliv. Rev.*, 2011, **63**, 300–311.

11 R. E. Unger, E. Dohle and C. J. Kirkpatrick, *Adv. Drug Deliv. Rev.*, 2015, **94**, 116–125.

12 X. Sun, W. Altalhi and S. S. Nunes, *Adv. Drug Deliv. Rev.*, 2016, **96**, 183–194.

13 S. V Lopes, M. N. Collins, R. L. Reis, J. M. Oliveira and J. Silva-Correia, *ACS Appl. Bio Mater.*, 2021, **4**, 2941–2956.

14 K. L. Spiller, R. R. Anfang, K. J. Spiller, J. Ng, K. R. Nakazawa, J. W. Daulton and G.

Vunjak-Novakovic, *Biomaterials*, 2014, **35**, 4477–4488.

15 L. E. Bertassoni, M. Cecconi, V. Manoharan, M. Nikkhah, J. Hjortnaes, A. L. Cristino, G. Barabaschi, D. Demarchi, M. R. Dokmeci, Y. Yang and A. Khademhosseini, *Lab Chip*, 2014, **14**, 2202–2211.

16 N. G. Schott, N. E. Friend and J. P. Stegemann, *Tissue Eng. Part B Rev.*, 2020, **27**, 199–214.

17 L. A. Herron, C. S. Hansen and H. E. Abaci, *Bioeng. Transl. Med.*, 2019, **4**, e10139.

18 E. A. Neuwelt, B. Bauer, C. Fahlke, G. Fricker, C. Iadecola, D. Janigro, L. Leybaert, Z. Molnár, M. E. O'Donnell, J. T. Povlishock, N. R. Saunders, F. Sharp, D. Stanimirovic, R. J. Watts and L. R. Drewes, *Nat. Rev. Neurosci.*, 2011, **12**, 169–182.

19 M. Potente and T. Mäkinen, *Nat. Rev. Mol. Cell Biol.*, 2017, **18**, 477–494.

20 Y. Serlin, I. Shelef, B. Knyazer and A. Friedman, *Semin. Cell Dev. Biol.*, 2015, **38**, 2–6.

21 S. Miyashima, J. Sebastian, J.-Y. Lee and Y. Helariutta, *EMBO J.*, 2013, **32**, 178–193.

22 M. Giannotta, M. Trani and E. Dejana, *Dev. Cell*, 2013, **26**, 441–454.

23 P. R. Kiela and F. K. Ghishan, *Best Pract. Res. Clin. Gastroenterol.*, 2016, **30**, 145–159.

24 W. Mertz, *Science*, 1981, **213**, 1332–1338.

25 C. Wanner, K. Amann and T. Shoji, *Lancet*, 2016, **388**, 276–284.

26 D. I. Brown and K. K. Griendling, *Circ. Res.*, 2015, **116**, 531–549.

27 M. K. Pugsley and R. Tabrizchi, *J. Pharmacol. Toxicol. Methods*, 2000, **44**, 333–340.

28 T. Winkler, F. A. Sass, G. N. Duda and K. Schmidt-Bleek, *Bone Joint Res.*, 2018, **7**, 232–243.

29 K. M. Galler, *Int. Endod. J.*, 2016, **49**, 926–936.

30 Z. Zhang, B. Wang, D. Hui, J. Qiu and S. Wang, *Compos. Part B Eng.*, 2017, **123**, 279–291.

31 C. Siebel and U. Lendahl, *Physiol. Rev.*, 2017, **97**, 1235–1294.

32 M. K. Rasmussen, H. Mestre and M. Nedergaard, *Physiol. Rev.*, 2021, **102**, 1025–1151.

33 A. D. Theocharis, S. S. Skandalis, C. Gialeli and N. K. Karamanos, *Adv. Drug Deliv. Rev.*, 2016, **97**, 4–27.

34 M. Xue, R. Zhao, H. Lin and C. Jackson, *Adv. Drug Deliv. Rev.*, 2018, **129**, 219–241.

35 E. A. Logsdon, S. D. Finley, A. S. Popel and F. Mac Gabhann, *J. Cell. Mol. Med.*, 2014, **18**, 1491–1508.

36 J. P. Straehla, C. Hajal, H. C. Safford, G. S. Offeddu, N. Boehnke, T. G. Dacoba, J. Wyckoff, R. D. Kamm and P. T. Hammond, *Proc. Natl. Acad. Sci.*, 2022, **119**, e2118697119.

37 L. Y. Daikuara, X. Chen, Z. Yue, D. Skropeta, F. M. Wood, M. W. Fear and G. G. Wallace, *Adv. Funct. Mater.*, 2022, **32**, 2105080.

38 H. Ravanbakhsh, V. Karamzadeh, G. Bao, L. Mongeau, D. Juncker and Y. S. Zhang, *Adv. Mater.*, 2021, **33**, 2104730.

39 J. M. Bliley, D. J. Shiwarski and A. W. Feinberg, *Sci. Transl. Med.*, 2023, **14**, eabo7047.

40 A. Hasan, A. Paul, N. E. Vrana, X. Zhao, A. Memic, Y.-S. Hwang, M. R. Dokmeci and A. Khademhosseini, *Biomaterials*, 2014, **35**, 7308–7325.

41 A. Sontheimer-Phelps, B. A. Hassell and D. E. Ingber, *Nat. Rev. Cancer*, 2019, **19**, 65–81.

42 T. Osaki, V. Sivathanu and R. D. Kamm, *Curr. Opin. Biotechnol.*, 2018, **52**, 116–123.

43 S. V Murphy, P. De Coppi and A. Atala, *Nat. Biomed. Eng.*, 2020, **4**, 370–380.

44 S. V Murphy and A. Atala, *Nat. Biotechnol.*, 2014, **32**, 773–785.

45 J. M. Ayuso, M. Virumbrales-Muñoz, J. M. Lang and D. J. Beebe, *Nat. Commun.*, 2022, **13**, 3086.

46 E. Garreta, R. D. Kamm, S. M. Chuva de Sousa Lopes, M. A. Lancaster, R. Weiss, X. Trepat, I. Hyun and N. Montserrat, *Nat. Mater.*, 2021, **20**, 145–155.

47 Y. Yu, L. Shang, J. Guo, J. Wang and Y. Zhao, *Nat. Protoc.*, 2018, **13**, 2557–2579.

48 M. Mao, X. Qu, Y. Zhang, B. Gu, C. Li, R. Liu, X. Li, H. Zhu, J. He and D. Li, *Nat. Commun.*, 2023, **14**, 2077.

49 L. Andrique, G. Recher, K. Alessandri, N. Pujol, M. Feyeux, P. Bon, L. Cognet, P. Nassoy and A. Bikfalvi, *Sci. Adv.*, 2023, **5**, eaau6562.

50 B. Kang, J. Shin, H.-J. Park, C. Rhyou, D. Kang, S.-J. Lee, Y. Yoon, S.-W. Cho and H. Lee, *Nat. Commun.*, 2018, **9**, 5402.

51 X. Ma, J. Liu, W. Zhu, M. Tang, N. Lawrence, C. Yu, M. Gou and S. Chen, *Adv. Drug Deliv. Rev.*, 2018, **132**, 235–251.

52 I. T. Ozbolat, *Trends Biotechnol.*, 2015, **33**, 395–400.

53 S. Vijayavenkataraman, W.-C. Yan, W. F. Lu, C.-H. Wang and J. Y. H. Fuh, *Adv. Drug Deliv. Rev.*, 2018, **132**, 296–332.

54 F. Mota, L. Braga, L. Rocha and B. Cabral, *Nat. Biotechnol.*, 2020, **38**, 689–694.

55 S. Cho, D. E. Discher, K. W. Leong, G. Vunjak-Novakovic and J. C. Wu, *Nat. Methods*, 2022, **19**, 1064–1071.

56 A. Gough, A. Soto-Gutierrez, L. Vernetti, M. R. Ebrahimkhani, A. M. Stern and D. L. Taylor, *Nat. Rev. Gastroenterol. Hepatol.*, 2021, **18**, 252–268.

57 I. Matai, G. Kaur, A. Seyedsalehi, A. McClinton and C. T. Laurencin, *Biomaterials*, 2020, **226**, 119536.

58 W. Sun, B. Starly, A. C. Daly, J. A. Burdick, J. Groll, G. Skeldon, W. Shu, Y. Sakai, M. Shinohara, M. Nishikawa, J. Jang, D.-W. Cho, M. Nie, S. Takeuchi, S. Ostrovidov, A. Khademhosseini, R. D. Kamm, V. Mironov, L. Moroni and I. T. Ozbolat, *Biofabrication*, 2020, **12**, 22002.

59 S. Sumantakul and V. T. Remcho, *Lab Chip*, 2023, **23**, 3194–3206.

60 I. Papautsky and E. T. K. Peterson, ed. D. Li, Springer US, Boston, MA, 2008, pp. 1256–1267.

61 D. Qin, Y. Xia and G. M. Whitesides, *Nat. Protoc.*, 2010, **5**, 491–502.

62 J. Bachmann, P. Obst, L. Knorr, S. Schmölzer, G. Fruhmann, G. Witt, T. Osswald, K. Wudy and O. Hinrichsen, *Commun. Mater.*, 2021, **2**, 107.

63 B. E. Kelly, I. Bhattacharya, H. Heidari, M. Shusteff, C. M. Spadaccini and H. K. Taylor, *Science*, 2019, **363**, 1075–1079.

64 E. M. Conway, D. Collen and P. Carmeliet, *Cardiovasc. Res.*, 2001, **49**, 507–521.

65 M. R. Swift and B. M. Weinstein, *Circ. Res.*, 2009, **104**, 576–588.

66 K. Alitalo, T. Tammela and T. V Petrova, *Nature*, 2005, **438**, 946–953.

67 G. N. Chaldakov, J. Beltowsky, P. I. Ghenev, M. Fiore, P. Panayotov, G. Rančič and L. Aloe, *Cell Biol. Int.*, 2012, **36**, 327–330.

68 B. F. Waller, C. M. Orr, J. D. Slack, C. A. Pinkerton, J. Van Tassel and T. Peters, *Clin. Cardiol.*, 1992, **15**, 451–457.

69 J. P. Travers, C. E. Brookes, J. Evans, D. M. Baker, C. Kent, G. S. Makin and T. M. Mayhew, *Eur. J. Vasc. Endovasc. Surg.*, 1996, **11**, 230–237.

70 P. Komutrattananont, P. Mahakkanukrauh and S. Das, *ACB*, 2019, **52**, 109–114.

71 C. Göktürk, J. Nilsson, J. Nordquist, M. Kristensson, K. Svensson, C. Söderberg, M. Israelson, H. Garpenstrand, M. Sjöquist, L. Oreland and K. Forsberg-Nilsson, *Am. J. Pathol.*, 2003, **163**, 1921–1928.

72 Y. Jeong, Y. Yao and E. K. F. Yim, *Biomater. Sci.*, 2020, **8**, 4383–4395.
73 C. P. Johnson, R. Baugh, C. A. Wilson and J. Burns, *J. Clin. Pathol.*, 2001, **54**, 139–145.
74 S. Y. Ho, J. A. Cabrera, V. H. Tran, J. Farré, R. H. Anderson and D. Sánchez-Quintana, *Heart*, 2001, **86**, 265–270.
75 H. S. Bennett, J. H. Luft and J. C. Hampton, *Am. J. Physiol. Content*, 1959, **196**, 381–390.
76 S. Nielsen, B. L. Smith, E. I. Christensen and P. Agre, *Proc. Natl. Acad. Sci.*, 1993, **90**, 7275–7279.
77 I. M. Braverman, *J. Investig. Dermatology Symp. Proc.*, 2000, **5**, 3–9.
78 H. Hashizume, P. Baluk, S. Morikawa, J. W. McLean, G. Thurston, S. Roberge, R. K. Jain and D. M. McDonald, *Am. J. Pathol.*, 2000, **156**, 1363–1380.
79 W. Groner, J. W. Winkelman, A. G. Harris, C. Ince, G. J. Bouma, K. Messmer and R. G. Nadeau, *Nat. Med.*, 1999, **5**, 1209–1212.
80 H. Latta, *J. Ultrastruct. Res.*, 1970, **32**, 526–544.
81 R. Vracko and E. P. Benditt, *J. Cell Biol.*, 1970, **47**, 281–285.
82 W. D. Tucker, Y. Arora and K. Mahajan, *Anatomy, Blood Vessels*, StatPearls Publishing, Treasure Island (FL), ETSU Quillen College of Medicine, 2022.
83 Y. M. Ju, J. S. Choi, A. Atala, J. J. Yoo and S. J. Lee, *Biomaterials*, 2010, **31**, 4313–4321.
84 G. I. De Jong, E. Farkas, C. M. Stienstra, J. R. M. Plass, J. N. Keijser, J. C. de la Torre and P. G. M. Luiten, *Neuroscience*, 1999, **91**, 203–210.
85 W. P. Paaske and P. Sejrsen, *Dan. Med. Bull.*, 1989, **36**, 570–590.
86 G. G. Maul, *J. Ultrastruct. Res.*, 1971, **36**, 768–782.
87 T. Kamba, B. Y. Y. Tam, H. Hashizume, A. Haskell, B. Sennino, M. R. Mancuso, S. M. Norberg, S. M. O'Brien, R. B. Davis, L. C. Gowen, K. D. Anderson, G. Thurston, S. Joho, M. L. Springer, C. J. Kuo and D. M. McDonald, *Am. J. Physiol. Circ. Physiol.*, 2006, **290**, 560–576.
88 F. Schaffner and H. Popper, *Gastroenterology*, 1963, **44**, 239–242.
89 J.-Y. Scoazec and G. Feldmann, *Hepatology*, 1991, **14**, 789–797.
90 S. Patel-Hett and P. D'Amore, *Int. J. Dev. Biol.*, 2011, **55**, 353–363.
91 W. Risau and I. Flamme, *Annu. Rev. Cell Dev. Biol.*, 1995, **11**, 73–91.
92 R. N. Feinberg and D. C. Beebe, *Science*, 1983, **220**, 1177–1179.
93 T. Shinoka, D. Shum-Tim, P. X. Ma, R. E. Tanel, N. Isogai, R. Langer, J. P. Vacanti and

J. E. Mayer, *J. Thorac. Cardiovasc. Surg.*, 1998, **115**, 536–546.

94 I. Leivo, A. Vaheri, R. Timpl and J. Wartiovaara, *Dev. Biol.*, 1980, **76**, 100–114.

95 D. Shook and R. Keller, *Mech. Dev.*, 2003, **120**, 1351–1383.

96 M. J. Ferkowicz and M. C. Yoder, *Exp. Hematol.*, 2005, **33**, 1041–1047.

97 K. Choi, *J. Hematother. Stem Cell Res.*, 2002, **11**, 91–101.

98 M. Kennedy, S. L. D'Souza, M. Lynch-Kattman, S. Schwantz and G. Keller, *Blood*, 2006, **109**, 2679–2687.

99 H. Naito, T. Iba and N. Takakura, *Int. Immunol.*, 2020, **32**, 295–305.

100 C. J. Drake, *Birth Defects Res. Part C Embryo Today Rev.*, 2003, **69**, 73–82.

101 S. J. Mentzer and M. A. Konerding, *Angiogenesis*, 2014, **17**, 499–509.

102 S. P. Herbert and D. Y. R. Stainier, *Nat. Rev. Mol. Cell Biol.*, 2011, **12**, 551–564.

103 N. Papadopoulos, J. Martin, Q. Ruan, A. Rafique, M. P. Rosconi, E. Shi, E. A. Pyles, G. D. Yancopoulos, N. Stahl and S. J. Wiegand, *Angiogenesis*, 2012, **15**, 171–185.

104 L. Jakobsson, C. A. Franco, K. Bentley, R. T. Collins, B. Ponsioen, I. M. Aspalter, I. Rosewell, M. Busse, G. Thurston, A. Medvinsky, S. Schulte-Merker and H. Gerhardt, *Nat. Cell Biol.*, 2010, **12**, 943–953.

105 F. Hillen and A. W. Griffioen, *Cancer Metastasis Rev.*, 2007, **26**, 489–502.

106 P. Kaufmann, T. M. Mayhew and D. S. Charnock-Jones, *Placenta*, 2004, **25**, 114–126.

107 D. W. Hutmacher, M. Sittinger and M. V Risbud, *Trends Biotechnol.*, 2004, **22**, 354–362.

108 S. J. Hollister, *Nat. Mater.*, 2005, **4**, 518–524.

109 D. W. Hutmacher, *J. Biomater. Sci. Polym. Ed.*, 2001, **12**, 107–124.

110 A. Eltom, G. Zhong and A. Muhammad, *Adv. Mater. Sci. Eng.*, 2019, **2019**, 3429527.

111 B. D. Ratner and S. J. Bryant, *Annu. Rev. Biomed. Eng.*, 2004, **6**, 41–75.

112 N. A. Peppas and R. Langer, *Science*, 1994, **263**, 1715–1720.

113 N. Huebsch and D. J. Mooney, *Nature*, 2009, **462**, 426–432.

114 Z. Chen, T. Klein, R. Z. Murray, R. Crawford, J. Chang, C. Wu and Y. Xiao, *Mater. Today*, 2016, **19**, 304–321.

115 L. S. Nair and C. T. Laurencin, *Prog. Polym. Sci.*, 2007, **32**, 762–798.

116 C. H. Lee, A. Singla and Y. Lee, *Int. J. Pharm.*, 2001, **221**, 1–22.

117 M. D. Shoulders and R. T. Raines, *Annu. Rev. Biochem.*, 2009, **78**, 929–958.

118 F. Croisier and C. Jérôme, *Eur. Polym. J.*, 2013, **49**, 780–792.

119 P. S. Bakshi, D. Selvakumar, K. Kadirvelu and N. S. Kumar, *Int. J. Biol. Macromol.*, 2020, **150**, 1072–1083.

120 K. Yue, G. Trujillo-de Santiago, M. M. Alvarez, A. Tamayol, N. Annabi and A. Khademhosseini, *Biomaterials*, 2015, **73**, 254–271.

121 M. Foox and M. Zilberman, *Expert Opin. Drug Deliv.*, 2015, **12**, 1547–1563.

122 J. F. Mano, G. A. Silva, H. S. Azevedo, P. B. Malafaya, R. A. Sousa, S. S. Silva, L. F. Boesel, J. M. Oliveira, T. C. Santos, A. P. Marques, N. M. Neves and R. L. Reis, *J. R. Soc. Interface*, 2007, **4**, 999–1030.

123 G. Chen, T. Ushida and T. Tateishi, *Macromol. Biosci.*, 2002, **2**, 67–77.

124 F.-M. Chen and X. Liu, *Prog. Polym. Sci.*, 2016, **53**, 86–168.

125 X. Liu and P. X. Ma, *Ann. Biomed. Eng.*, 2004, **32**, 477–486.

126 E. S. Place, J. H. George, C. K. Williams and M. M. Stevens, *Chem. Soc. Rev.*, 2009, **38**, 1139–1151.

127 A. Bharadwaz and A. C. Jayasuriya, *Mater. Sci. Eng. C*, 2020, **110**, 110698.

128 G. D. Mogoşanu and A. M. Grumezescu, *Int. J. Pharm.*, 2014, **463**, 127–136.

129 A. Sionkowska, *Prog. Polym. Sci.*, 2011, **36**, 1254–1276.

130 P. Gunatillake, R. Mayadunne and R. Adhikari, *Biotechnol. Annu. Rev.*, 2006, **12**, 301–347.

131 M. F. Maitz, *Biosurface and Biotribology*, 2015, **1**, 161–176.

132 Z. Wang, H. Wei, Y. Huang, Y. Wei and J. Chen, *Chem. Soc. Rev.*, 2023, **52**, 2992–3034.

133 Z. Wang, M. Heck, W. Yang, M. Wilhelm and P. A. Levkin, *Adv. Funct. Mater.*, 2023, **n/a**, 2300947.

134 Y. S. Zhang and A. Khademhosseini, *Science*, 2017, **356**, eaaf3627.

135 M. N. Collins, G. Ren, K. Young, S. Pina, R. L. Reis and J. M. Oliveira, *Adv. Funct. Mater.*, 2021, **31**, 2010609.

136 P. S. Gungor-Ozkerim, I. Inci, Y. S. Zhang, A. Khademhosseini and M. R. Dokmeci, *Biomater. Sci.*, 2018, **6**, 915–946.

137 G. M. Whitesides, *Nature*, 2006, **442**, 368–373.

138 E. K. Sackmann, A. L. Fulton and D. J. Beebe, *Nature*, 2014, **507**, 181–189.

139 G. Simitian, M. Virumbrales-Muñoz, C. Sánchez-de-Diego, D. J. Beebe and D. Kosoff,

Lab Chip, 2022, **22**, 3618–3636.

140 J. Ko, J. Ahn, S. Kim, Y. Lee, J. Lee, D. Park and N. L. Jeon, *Lab Chip*, 2019, **19**, 2822–2833.

141 Y. Xia and G. M. Whitesides, *Annu. Rev. Mater. Sci.*, 1998, **28**, 153–184.

142 S. Brittain, K. Paul, X.-M. Zhao and G. Whitesides, *Phys. World*, 1998, **11**, 31.

143 M. A. Unger, H.-P. Chou, T. Thorsen, A. Scherer and S. R. Quake, *Science*, 2000, **288**, 113–116.

144 A. del Campo and E. Arzt, *Chem. Rev.*, 2008, **108**, 911–945.

145 G. M. Whitesides, E. Ostuni, S. Takayama, X. Jiang and D. E. Ingber, *Annu. Rev. Biomed. Eng.*, 2001, **3**, 335–373.

146 J. A. Rogers and R. G. Nuzzo, *Mater. Today*, 2005, **8**, 50–56.

147 N. S. G. K. Devaraju and M. A. Unger, *Lab Chip*, 2012, **12**, 4809–4815.

148 J. P. Rolland, E. C. Hagberg, G. M. Denison, K. R. Carter and J. M. De Simone, *Angew. Chemie Int. Ed.*, 2004, **43**, 5796–5799.

149 K. M. Choi and J. A. Rogers, *J. Am. Chem. Soc.*, 2003, **125**, 4060–4061.

150 H.-S. Noh, Y. Huang and P. J. Hesketh, *Sensors Actuators B Chem.*, 2004, **102**, 78–85.

151 M Heckele and W K Schomburg, *J. Micromechanics Microengineering*, 2004, **14**, R1.

152 J. Giboz, T. Copponnex and P. Mélé, *J. Micromechanics Microengineering*, 2007, **17**, R96.

153 J. S. Jeon, S. Chung, R. D. Kamm and J. L. Charest, *Biomed. Microdevices*, 2011, **13**, 325–333.

154 B.-B. Xu, Y.-L. Zhang, H. Xia, W.-F. Dong, H. Ding and H.-B. Sun, *Lab Chip*, 2013, **13**, 1677–1690.

155 J. Gim and L.-S. Turng, *Polym. Test.*, 2022, **115**, 107718.

156 J. Schellenberg and H.-J. Leder, *Adv. Polym. Technol.*, 2006, **25**, 141–151.

157 M. Yamazaki, *J. Mol. Catal. A Chem.*, 2004, **213**, 81–87.

158 S. S. Deshmukh and A. Goswami, *Mater. Today Proc.*, 2020, **26**, 405–414.

159 S. S. Deshmukh and A. Goswami, *Mater. Manuf. Process.*, 2021, **36**, 501–543.

160 S. Ravi-Kumar, B. Lies, X. Zhang, H. Lyu and H. Qin, *Polym. Int.*, 2019, **68**, 1391–1401.

161 H. Wang, Y.-L. Zhang, W. Wang, H. Ding and H.-B. Sun, *Laser Photon. Rev.*, 2017, **11**, 1600116.

162 A. G. Bondarenko, A. Ramos-Velazquez, A. V Shmalko and R. A. Zakoldaev, *Opt. Quantum Electron.*, 2023, **55**, 379.

163 J.-W. Chen, J. Zybko and J. Clements, *MRS Online Proc. Libr.*, 2005, **872**, J15.6.

164 G. B. Blanchet and S. I. Shah, *Appl. Phys. Lett.*, 1993, **62**, 1026–1028.

165 C. De Marco, S. M. Eaton, R. Suriano, S. Turri, M. Levi, R. Ramponi, G. Cerullo and R. Osellame, *ACS Appl. Mater. Interfaces*, 2010, **2**, 2377–2384.

166 N. Ahmed, S. Darwish and A. M. Alahmari, *Mater. Manuf. Process.*, 2016, **31**, 1121–1142.

167 M. A. Roberts, D. Tran, K. L. K. Coulombe, M. Razumova, M. Regnier, C. E. Murry and Y. Zheng, *Tissue Eng. Part A*, 2016, **22**, 633–644.

168 F. Chesnais, J. Joel, J. Hue, S. Shakib, L. Di Silvio, A. E. Grigoriadis, T. Coward and L. Veschini, *Lab Chip*, 2023, **23**, 761–772.

169 Y. Zheng, J. Chen, M. Craven, N. W. Choi, S. Totorica, A. Diaz-Santana, P. Kermani, B. Hempstead, C. Fischbach-Teschl, J. A. López and A. D. Stroock, *Proc. Natl. Acad. Sci.*, 2012, **109**, 9342–9347.

170 A. E. Emerson, A. B. McCall, S. R. Brady, E. M. Slaby and J. D. Weaver, *ACS Biomater. Sci. Eng.*, 2022, **8**, 4002–4013.

171 M. A. Redd, N. Zeinstra, W. Qin, W. Wei, A. Martinson, Y. Wang, R. K. Wang, C. E. Murry and Y. Zheng, *Nat. Commun.*, 2019, **10**, 584.

172 W. Asghar, R. El Assal, H. Shafiee, S. Pitteri, R. Paulmurugan and U. Demirci, *Mater. Today*, 2015, **18**, 539–553.

173 Y. Kim, J. Ko, N. Shin, S. Park, S.-R. Lee, S. Kim, J. Song, S. Lee, K.-S. Kang, J. Lee and N. L. Jeon, *Biotechnol. Bioeng.*, 2022, **119**, 3678–3693.

174 X. Wang, M. R. Salick, Y. Gao, J. Jiang, X. Li, F. Liu, T. Cordie, Q. Li and L.-S. Turng, *J. Cell. Plast.*, 2016, **54**, 379–397.

175 L. Peng, Y. Deng, P. Yi and X. Lai, *J. Micromechanics Microengineering*, 2014, **24**, 13001.

176 B. F. L. Lai, R. X. Z. Lu, L. Davenport Huyer, S. Kakinoki, J. Yazbeck, E. Y. Wang, Q. Wu, B. Zhang and M. Radisic, *Nat. Protoc.*, 2021, **16**, 2158–2189.

177 B. F. L. Lai, R. X. Z. Lu, Y. Hu, L. Davenport Huyer, W. Dou, E. Y. Wang, N. Radulovich, M. S. Tsao, Y. Sun and M. Radisic, *Adv. Funct. Mater.*, 2020, **30**, 2000545.

178 B. Aor, I. Khan, K. Glinel, A. M. Jonas, S. Demoustier-Champagne and M.-C. Durrieu, *ACS Appl. Bio Mater.*, 2020, **3**, 1520–1532.

179 A. M. Leferink, M. P. Tibbe, E. G. B. M. Bossink, L. E. de Heus, H. van Vossen, A. van den Berg, L. Moroni and R. K. Truckenmüller, *Mater. Today Bio*, 2019, **4**, 100025.

180 M. Duchamp, S. M. Bakht, J. Ju, I. K. Yazdi, W. Zhang and Y. S. Zhang, *Adv. Mater. Technol.*, 2019, **4**, 1800741.

181 C. F. Bellani, K. Yue, F. Flaig, A. Hébraud, P. Ray, N. Annabi, H. S. Selistre de Araújo, M. C. Branciforti, A. M. Minarelli Gaspar, S. R. Shin, A. Khademhosseini and G. Schlatter, *Biofabrication*, 2021, **13**, 35020.

182 B. Buchroithner, S. Mayr, F. Hauser, E. Priglinger, H. Stangl, A. R. Santa-Maria, M. A. Deli, A. Der, T. A. Klar, M. Axmann, D. Sivun, M. Mairhofer and J. Jacak, *ACS Nano*, 2021, **15**, 2984–2993.

183 A. Tevlek, B. Topuz, E. Akbay and H. M. Aydin, *J. Biomater. Appl.*, 2022, **37**, 287–302.

184 B. Derby, *J. Mater. Chem.*, 2008, **18**, 5717–5721.

185 X. Li, B. Liu, B. Pei, J. Chen, D. Zhou, J. Peng, X. Zhang, W. Jia and T. Xu, *Chem. Rev.*, 2020, **120**, 10793–10833.

186 X. Cui and T. Boland, *Biomaterials*, 2009, **30**, 6221–6227.

187 H. Wijshoff, *Phys. Rep.*, 2010, **491**, 77–177.

188 K. H. Choi, A. Ali, A. Rahman, N. Malik Mohammad, K. Rahman, A. Khan, S. Khan and D. S. Kim, *J. Micromechanics Microengineering*, 2010, **20**, 75033.

189 G. Mattana, A. Loi, M. Woytasik, M. Barbaro, V. Noël and B. Piro, *Adv. Mater. Technol.*, 2017, **2**, 1700063.

190 J. L. Hoehne, R. Carlstron, J. Dernorwsek, P. C. Cristovam, H. L. Bachiega, S. I. Abensur and P. Schor, *Biomed. Phys. Eng. Express*, 2020, **6**, 35021.

191 H. Gudapati, M. Dey and I. Ozbolat, *Biomaterials*, 2016, **102**, 20–42.

192 I. T. Ozbolat and M. Hospodiuk, *Biomaterials*, 2016, **76**, 321–343.

193 X. Cui, J. Li, Y. Hartanto, M. Durham, J. Tang, H. Zhang, G. Hooper, K. Lim and T. Woodfield, *Adv. Healthc. Mater.*, 2020, **9**, 1901648.

194 S. Ji and M. Guvendiren, *Front. Bioeng. Biotechnol.*, 2017, 5, 23.

195 S. Kyle, Z. M. Jessop, A. Al-Sabah and I. S. Whitaker, *Adv. Healthc. Mater.*, 2017, **6**, 1700264.

196 J. K. Placone and A. J. Engler, *Adv. Healthc. Mater.*, 2018, **7**, 1701161.

197 W. Liu, M. A. Heinrich, Y. Zhou, A. Akpek, N. Hu, X. Liu, X. Guan, Z. Zhong, X. Jin, A. Khademhosseini and Y. S. Zhang, *Adv. Healthc. Mater.*, 2017, **6**, 1601451.

198 K. Zhu, N. Chen, X. Liu, X. Mu, W. Zhang, C. Wang and Y. S. Zhang, *Macromol. Biosci.*, 2018, **18**, 1800127.

199 L. Ouyang, J. P. K. Armstrong, Y. Lin, J. P. Wojciechowski, C. Lee-Reeves, D. Hachim, K. Zhou, J. A. Burdick and M. M. Stevens, *Sci. Adv.*, 2024, **6**, eabc5529.

200 K. T. Lawlor, J. M. Vanslambrouck, J. W. Higgins, A. Chambon, K. Bishard, D. Arndt, P. X. Er, S. B. Wilson, S. E. Howden, K. S. Tan, F. Li, L. J. Hale, B. Shepherd, S. Pentoney, S. C. Presnell, A. E. Chen and M. H. Little, *Nat. Mater.*, 2021, **20**, 260–271.

201 T. J. Hinton, Q. Jallerat, R. N. Palchesko, J. H. Park, M. S. Grodzicki, H.-J. Shue, M. H. Ramadan, A. R. Hudson and A. W. Feinberg, *Sci. Adv.*, 2023, **1**, e1500758.

202 F. P. W. Melchels, J. Feijen and D. W. Grijpma, *Biomaterials*, 2010, **31**, 6121–6130.

203 R. L. Truby and J. A. Lewis, *Nature*, 2016, **540**, 371–378.

204 M. Lee, R. Rizzo, F. Surman and M. Zenobi-Wong, *Chem. Rev.*, 2020, **120**, 10950–11027.

205 R. Levato, O. Dudaryeva, C. E. Garciamendez-Mijares, B. E. Kirkpatrick, R. Rizzo, J. Schimelman, K. S. Anseth, S. Chen, M. Zenobi-Wong and Y. S. Zhang, *Nat. Rev. Methods Prim.*, 2023, **3**, 47.

206 O. Santoliquido, P. Colombo and A. Ortona, *J. Eur. Ceram. Soc.*, 2019, **39**, 2140–2148.

207 B. Zhao, J. Li, G. Li, X. Yang, S. Lu, X. Pan and J. Zhu, *Small*, 2023, **n/a**, 2207637.

208 A. Quaak, Q. Thijssen and S. Van Vlierberghe, *Polym. Chem.*, 2023, **14**, 3392–3403.

209 I. Chiulan, E. B. Heggset, Ş. I. Voicu and G. Chinga-Carrasco, *Biomacromolecules*, 2021, **22**, 1795–1814.

210 H. Quan, T. Zhang, H. Xu, S. Luo, J. Nie and X. Zhu, *Bioact. Mater.*, 2020, **5**, 110–115.

211 S. H. Kim, H. Hong, O. Ajiteru, M. T. Sultan, Y. J. Lee, J. S. Lee, O. J. Lee, H. Lee, H. S. Park, K. Y. Choi, J. S. Lee, H. W. Ju, I.-S. Hong and C. H. Park, *Nat. Protoc.*, 2021, **16**, 5484–5532.

212 Q. Mao, Y. Wang, Y. Li, S. Juengpanich, W. Li, M. Chen, J. Yin, J. Fu and X. Cai, *Mater. Sci. Eng. C*, 2020, **109**, 110625.

213 D. Loterie, P. Delrot and C. Moser, *Nat. Commun.*, 2020, **11**, 852.

214 M. Regehly, Y. Garmshausen, M. Reuter, N. F. König, E. Israel, D. P. Kelly, C.-Y. Chou,

K. Koch, B. Asfari and S. Hecht, *Nature*, 2020, **588**, 620–624.

215 M. P. de Beer, H. L. van der Laan, M. A. Cole, R. J. Whelan, M. A. Burns and T. F. Scott, *Sci. Adv.*, 2024, **5**, eaau8723.

216 M. Xie, L. Lian, X. Mu, Z. Luo, C. E. Garciamendez-Mijares, Z. Zhang, A. López, J. Manríquez, X. Kuang, J. Wu, J. K. Sahoo, F. Z. González, G. Li, G. Tang, S. Maharjan, J. Guo, D. L. Kaplan and Y. S. Zhang, *Nat. Commun.*, 2023, **14**, 210.

217 C. Dou, V. Perez, J. Qu, A. Tsin, B. Xu and J. Li, *ChemBioEng Rev.*, 2021, **8**, 517–534.

218 D. J. Odde and M. J. Renn, *Biotechnol. Bioeng.*, 2000, **67**, 312–318.

219 B. T. Vinson, S. C. Sklare and D. B. Chrisey, *Curr. Opin. Biomed. Eng.*, 2017, **2**, 14–21.

220 E. Stratakis, A. Ranella and C. Fotakis, eds. V. Schmidt and M. R. Belegratis, Springer Berlin Heidelberg, Berlin, Heidelberg, 2013, pp. 211–236.

221 A. Zennifer, A. Subramanian and S. Sethuraman, *Bioprinting*, 2022, **27**, e00205.

222 A. Blaeser, D. F. Duarte Campos and H. Fischer, *Curr. Opin. Biomed. Eng.*, 2017, **2**, 58–66.

223 N. V Vitanov, T. Halfmann, B. W. Shore and K. Bergmann, *Annu. Rev. Phys. Chem.*, 2001, **52**, 763–809.

224 P. Serra and A. Piqué, *Adv. Mater. Technol.*, 2019, **4**, 1800099.

225 F. Guillemot, A. Souquet, S. Catros, B. Guillotin, J. Lopez, M. Faucon, B. Pippenger, R. Bareille, M. Rémy, S. Bellance, P. Chabassier, J. C. Fricain and J. Amédée, *Acta Biomater.*, 2010, **6**, 2494–2500.

226 V. Yusupov, S. Churbanov, E. Churbanova, K. Bardakova, A. Antoshin, S. Evlashin, P. Timashev and N. Minaev, *IJB*, **6**, 271.

227 M. Makrygianni, A. Milionis, C. Kryou, I. Trantakis, D. Poulikakos and I. Zergioti, *Adv. Mater. Interfaces*, 2018, **5**, 1800440.

228 F. Guillemot, A. Souquet, S. Catros and B. Guillotin, *Nanomedicine*, 2010, **5**, 507–515.

229 A. Sorkio, L. Koch, L. Koivusalo, A. Deiwick, S. Miettinen, B. Chichkov and H. Skottman, *Biomaterials*, 2018, **171**, 57–71.

230 V. Keriquel, H. Oliveira, M. Rémy, S. Ziane, S. Delmond, B. Rousseau, S. Rey, S. Catros, J. Amédée, F. Guillemot and J.-C. Fricain, *Sci. Rep.*, 2017, **7**, 1778.

231 C. Douillet, M. Nicodeme, L. Hermant, V. Bergeron, F. Guillemot, J.-C. Fricain, H. Oliveira and M. Garcia, *Biofabrication*, 2022, **14**, 25006.

232 F. Zheng, B. Derby and J. Wong, *Biofabrication*, 2021, **13**, 35006.

233 M. Matsusaki, H. Ikeguchi, C. Kubo, H. Sato, Y. Kuramochi and D. Takagi, *ACS Biomater. Sci. Eng.*, 2019, **5**, 5637–5643.

234 L. De Moor, J. Smet, M. Plovyt, B. Bekaert, C. Vercruysse, M. Asadian, N. De Geyter, S. Van Vlierberghe, P. Dubruel and H. Declercq, *Biofabrication*, 2021, **13**, 45021.

235 R. Hooper, C. Cummings, A. Beck, J. Vazquez-Armendariz, C. Rodriguez and D. Dean, *Biofabrication*, 2024, **16**, 25032.

236 Y. Fang, Y. Guo, B. Wu, Z. Liu, M. Ye, Y. Xu, M. Ji, L. Chen, B. Lu, K. Nie, Z. Wang, J. Luo, T. Zhang, W. Sun and Z. Xiong, *Adv. Mater.*, 2023, **35**, 2205082.

237 D. Wu, S. Pang, J. Berg, Y. Mei, A. S. M. Ali, V. Röhrs, B. Tolksdorf, J. Hagenbuchner, M. J. Ausserlechner, H. E. Deubzer, A. Gurlo and J. Kurreck, *Adv. Funct. Mater.*, 2024, **n/a**, 2314171.

238 A. Thomas, I. Orellano, T. Lam, B. Noichl, M.-A. Geiger, A.-K. Amler, A.-E. Kreuder, C. Palmer, G. Duda, R. Lauster and L. Kloke, *Acta Biomater.*, 2020, **117**, 121–132.

239 S. Wadnap, S. Krishnamoorthy, Z. Zhang and C. Xu, *J. Mater. Sci. Mater. Med.*, 2019, **30**, 36.

240 N. Anandakrishnan, H. Ye, Z. Guo, Z. Chen, K. I. Mentkowski, J. K. Lang, N. Rajabian, S. T. Andreadis, Z. Ma, J. A. Spernyak, J. F. Lovell, D. Wang, J. Xia, C. Zhou and R. Zhao, *Adv. Healthc. Mater.*, 2021, **10**, 2002103.

241 I. S. Kinstlinger and J. S. Miller, *Lab Chip*, 2016, **16**, 2025–2043.

242 H. Goodarzi Hosseinabadi, D. Nieto, A. Yousefinejad, H. Fattel, L. Ionov and A. K. Miri, *Appl. Mater. Today*, 2023, **30**, 101721.

243 C. Yu, J. Schimelman, P. Wang, K. L. Miller, X. Ma, S. You, J. Guan, B. Sun, W. Zhu and S. Chen, *Chem. Rev.*, 2020, **120**, 10695–10743.

244 W. Li, L. S. Mille, J. A. Robledo, T. Uribe, V. Huerta and Y. S. Zhang, *Adv. Healthc. Mater.*, 2020, **9**, 2000156.

245 G. S. Hussey, J. L. Dziki and S. F. Badylak, *Nat. Rev. Mater.*, 2018, **3**, 159–173.

246 S. P. Parthiban, A. Athirasala, A. Tahayeri, R. Abdelmoniem, A. George and L. E. Bertassoni, *Biofabrication*, 2021, **13**, 35031.

247 V. T. Duong and C.-C. Lin, *Macromol. Biosci.*, 2023, **n/a**, 2300213.

248 S. Goel and K. Amreen, *Biomicrofluidics*, 2022, **16**, 61505.

249 H. Petite, V. Viateau, W. Bensaïd, A. Meunier, C. de Pollak, M. Bourguignon, K. Oudina, L. Sedel and G. Guillemin, *Nat. Biotechnol.*, 2000, **18**, 959–963.

250 O. Kérourédan, J.-M. Bourget, M. Rémy, S. Crauste-Manciet, J. Kalisky, S. Catros, N. B. Thébaud and R. Devillard, *J. Mater. Sci. Mater. Med.*, 2019, **30**, 28.

251 F. Kawecki, W. P. Clafshenkel, F. A. Auger, J.-M. Bourget, J. Fradette and R. Devillard, *Biofabrication*, 2018, **10**, 35006.

252 S. Fleischer, D. N. Tavakol and G. Vunjak-Novakovic, *Adv. Funct. Mater.*, 2020, **30**, 1910811.

253 S. Gimondi, H. Ferreira, R. L. Reis and N. M. Neves, *ACS Nano*, 2023, **17**, 14205–14228.

254 P. A. Wieringa, A. R. Gonçalves de Pinho, S. Micera, R. J. A. van Wezel and L. Moroni, *Adv. Healthc. Mater.*, 2018, **7**, 1701164.

255 I. C. McLean, L. A. Schwerdtfeger, S. A. Tobet and C. S. Henry, *Lab Chip*, 2018, **18**, 1399–1410.

256 C. O'Connor, E. Brady, Y. Zheng, E. Moore and K. R. Stevens, *Nat. Rev. Mater.*, 2022, **7**, 702–716.

257 M. L. Bedell, A. M. Navara, Y. Du, S. Zhang and A. G. Mikos, *Chem. Rev.*, 2020, **120**, 10744–10792.

258 P. Wang, Y. Sun, X. Shi, H. Shen, H. Ning and H. Liu, *Bio-Design Manuf.*, 2021, **4**, 344–378.

259 C. Mota, S. Camarero-Espinosa, M. B. Baker, P. Wieringa and L. Moroni, *Chem. Rev.*, 2020, **120**, 10547–10607.

260 A. Shapira and T. Dvir, *Adv. Sci.*, 2021, **8**, 2003751.

261 B. Zhang, Y. Luo, L. Ma, L. Gao, Y. Li, Q. Xue, H. Yang and Z. Cui, *Bio-Design Manuf.*, 2018, **1**, 2–13.

262 X. Meng, Y. Xing, J. Li, C. Deng, Y. Li, X. Ren and D. Zhang, *Front. Cell Dev. Biol.*, 2021, 9, 639299.

263 M. Lovett, K. Lee, A. Edwards and D. L. Kaplan, *Tissue Eng. Part B Rev.*, 2009, **15**, 353–370.

264 F. Yu and D. Choudhury, *Drug Discov. Today*, 2019, **24**, 1248–1257.

265 N. Tabatabaei Rezaei, H. Kumar, H. Liu, S. S. Lee, S. S. Park and K. Kim, *Adv. Healthc. Mater.*, 2023, **12**, 2203172.

266 K. S. Lim, M. Baptista, S. Moon, T. B. F. Woodfield and J. Rnjak-Kovacina, *Trends Biotechnol.*, 2019, **37**, 1189–1201.

267 J. Radhakrishnan, S. Varadaraj, S. K. Dash, A. Sharma and R. S. Verma, *Drug Discov. Today*, 2020, **25**, 879–890.

268 A. M. Jorgensen, J. J. Yoo and A. Atala, *Chem. Rev.*, 2020, **120**, 11093–11127.

269 N. Bhattacharjee, A. Urrios, S. Kang and A. Folch, *Lab Chip*, 2016, **16**, 1720–1742.

270 M. Matsusaki, K. Sakaue, K. Kadowaki and M. Akashi, *Adv. Healthc. Mater.*, 2013, **2**, 534–539.

271 J. Zhang, F. Chen, Z. He, Y. Ma, K. Uchiyama and J.-M. Lin, *Analyst*, 2016, **141**, 2940–2947.

272 N. S. Bhise, V. Manoharan, S. Massa, A. Tamayol, M. Ghaderi, M. Miscuglio, Q. Lang, Y. Shrike Zhang, S. R. Shin, G. Calzone, N. Annabi, T. D. Shupe, C. E. Bishop, A. Atala, M. R. Dokmeci and A. Khademhosseini, *Biofabrication*, 2016, **8**, 14101.

273 C. Colosi, S. R. Shin, V. Manoharan, S. Massa, M. Costantini, A. Barbetta, M. R. Dokmeci, M. Dentini and A. Khademhosseini, *Adv. Mater.*, 2016, **28**, 677–684.

274 E. Davoodi, E. Sarikhani, H. Montazerian, S. Ahadian, M. Costantini, W. Swieszkowski, S. M. Willerth, K. Walus, M. Mofidfar, E. Toyserkani, A. Khademhosseini and N. Ashammakhi, *Adv. Mater. Technol.*, 2020, **5**, 1901044.

275 G. Gao, J. Y. Park, B. S. Kim, J. Jang and D.-W. Cho, *Adv. Healthc. Mater.*, 2018, **7**, 1801102.

276 S. C. Millik, A. M. Dostie, D. G. Karis, P. T. Smith, M. McKenna, N. Chan, C. D. Curtis, E. Nance, A. B. Theberge and A. Nelson, *Biofabrication*, 2019, **11**, 45009.

277 W. Liu, Z. Zhong, N. Hu, Y. Zhou, L. Maggio, A. K. Miri, A. Fragasso, X. Jin, A. Khademhosseini and Y. S. Zhang, *Biofabrication*, 2018, **10**, 24102.

278 Q. Pi, S. Maharjan, X. Yan, X. Liu, B. Singh, A. M. van Genderen, F. Robledo-Padilla, R. Parra-Saldivar, N. Hu, W. Jia, C. Xu, J. Kang, S. Hassan, H. Cheng, X. Hou, A. Khademhosseini and Y. S. Zhang, *Adv. Mater.*, 2018, **30**, 1706913.

279 L. E. Niklason and J. H. Lawson, *Science*, 2020, **370**, eaaw8682.

280 D. Wang, S. Maharjan, X. Kuang, Z. Wang, L. S. Mille, M. Tao, P. Yu, X. Cao, L. Lian, L. Lv, J. J. He, G. Tang, H. Yuk, C. K. Ozaki, X. Zhao and Y. S. Zhang, *Sci. Adv.*, 2023, **8**, eabq6900.

281 A. Dellaquila, C. Le Bao, D. Letourneur and T. Simon-Yarza, *Adv. Sci.*, 2021, **8**, 2100798.

282 R. W. Barrs, J. Jia, S. E. Silver, M. Yost and Y. Mei, *Chem. Rev.*, 2020, **120**, 10887–10949.

283 J. Gong, C. C. L. Schuurmans, A. M. van Genderen, X. Cao, W. Li, F. Cheng, J. J. He, A. López, V. Huerta, J. Manríquez, R. Li, H. Li, C. Delavaux, S. Sebastian, P. E. Capendale, H. Wang, J. Xie, M. Yu, R. Masereeuw, T. Vermonden and Y. S. Zhang, *Nat. Commun.*, 2020, **11**, 1267.

284 G. Tang, Z. Luo, L. Lian, J. Guo, S. Maharjan, C. E. Garciamendez-Mijares, M. Wang, W. Li, Z. Zhang, D. Wang, M. Xie, H. Ravanbakhsh, C. Zhou, X. Kuang, Y. Hou, X. Yu and Y. S. Zhang, *Proc. Natl. Acad. Sci.*, 2023, **120**, e2206762120.

285 P. P. Stankey, K. T. Kroll, A. J. Ainscough, D. S. Reynolds, A. Elamine, B. T. Fichtenkort, S. G. M. Uzel and J. A. Lewis, *bioRxiv*, 2024, 2024.01.27.577581.

286 D. Kang, G. Hong, S. An, I. Jang, W.-S. Yun, J.-H. Shim and S. Jin, *Small*, 2020, **16**, 1905505.

287 D. Kang, G. Ahn, D. Kim, H.-W. Kang, S. Yun, W.-S. Yun, J.-H. Shim and S. Jin, *Biofabrication*, 2018, **10**, 35008.

288 M. Hospodiuk, M. Dey, D. Sosnoski and I. T. Ozbolat, *Biotechnol. Adv.*, 2017, **35**, 217–239.

289 A. K. Miri, D. Nieto, L. Iglesias, H. Goodarzi Hosseinabadi, S. Maharjan, G. U. Ruiz-Esparza, P. Khoshakhlagh, A. Manbachi, M. R. Dokmeci, S. Chen, S. R. Shin, Y. S. Zhang and A. Khademhosseini, *Adv. Mater.*, 2018, **30**, 1800242.

290 M. Wang, W. Li, L. S. Mille, T. Ching, Z. Luo, G. Tang, C. E. Garciamendez, A. Lesha, M. Hashimoto and Y. S. Zhang, *Adv. Mater.*, 2022, **34**, 2107038.

291 Y. Wu, H. Su, M. Li and H. Xing, *J. Biomed. Mater. Res. Part A*, 2023, **111**, 527–542.

292 H. Su, B. Lu, M. Li, X. Yang, M. Qin and Y. Wu, *Biomater. Sci.*, 2023, **11**, 6663–6673.

293 J. Liu, H. H. Hwang, P. Wang, G. Whang and S. Chen, *Lab Chip*, 2016, **16**, 1430–1438.

294 P. Weber, L. Cai, F. J. A. Rojas, C. E. Garciamendez-Mijares, M. C. Tirelli, F. Nalin, J. Jaroszewicz, W. Święszkowski, M. Costantini and Y. S. Zhang, *Aggregate*, 2024, **5**, e409.

295 J. Halper, in *Vascular Pharmacology: Cytoskeleton and Extracellular Matrix*, ed. R. A. B. T.-A. in P. Khalil, Academic Press, 2018, vol. 81, pp. 95–127.

296 S. You, Y. Xiang, H. H. Hwang, D. B. Berry, W. Kiratitanaporn, J. Guan, E. Yao, M.

Tang, Z. Zhong, X. Ma, D. Wangpraseurt, Y. Sun, T. Lu and S. Chen, *Sci. Adv.*, 2024, **9**, eade7923.

No primary research results, software or code have been included and no new data were generated or analysed as part of this review.